https://doi.org/10.5194/egusphere-2026-3284
Preprint. Discussion started: 19 June 2026

Structural Complexity and Preferential Flowpaths Govern Connectivity and DOC Export in a Remote Boreal Headwater Peatland Complex

Nicole Balliston[1,2], Julia Hathaway[3], Marianne Vogel[3], Sarah Finkelstein[3], Maria Strack[2]

[1]School of Natural Sciences, Laurentian University, Sudbury, Ontario, Canada
[2]Department of Geography and Environmental Management, University of Waterloo, Waterloo, Ontario, Canada
[3]Department of Earth Sciences, University of Toronto, Toronto, Ontario, Canada

Correspondence to: Nicole Balliston (nballiston@laurentian.ca)

Abstract. Northern peatlands store globally significant carbon stocks and are major sources of dissolved organic carbon (DOC) to downstream waters, yet the hydrological mechanisms controlling water and carbon export remain poorly resolved. This uncertainty is particularly important in structurally complex landscapes where wetland type, peat thickness, and mineral substrate properties shift over short distances, potentially creating localized but highly connected flowpaths that are difficult to capture in landscape-scale models and monitoring frameworks. Here, hydrological conditions, geochemistry, and DOC concentrations were monitored over two growing seasons across a peatland–lake transition in Canada's Precambrian Shield and integrated with subsurface flowpath modelling to determine how landscape structure and flowpath activation regulate water and DOC export.

Flowpath geometry remained stable despite substantial variation in water availability, indicating strong structural control by landscape morphology and subsurface properties. In contrast, water table dynamics varied among landscape units, constraining near-surface flowpath activation. Limited near-surface connectivity in upgradient wetlands was insufficient to explain persistent groundwater discharge at the outlet. Instead, evidence supports preferential subsurface flowpaths linking upgradient peatland units to a groundwater spring, sustaining discharge and episodically mobilizing DOC-rich waters. Catchment-scale annual DOC export to the downgradient lake was estimated between 3.1 and 14.1 g C m^{-2} yr^{-1}. More than 20% of this DOC export originated from the single groundwater spring, demonstrating that small, preferentially connected areas can exert disproportionate control on peatland carbon loss to downstream aquatic ecosystems. These findings suggest that predicting aquatic carbon export from northern peatlands under climate change and land-use disturbance requires greater attention to subsurface structure, threshold-mediated connectivity, and localized flowpaths that may be overlooked when peatlands are treated as spatially uniform source areas.

1.0 Introduction

Peatlands are globally significant carbon reservoirs, storing up to one-third of the world's terrestrial soil carbon despite covering only ~3% of the Earth's land surface (Limpens et al., 2008). In northern boreal landscapes, peatlands serve as long-term carbon sinks, but they are also dynamic sources of dissolved organic carbon (DOC) to downstream aquatic systems (Prijac et al., 2023; Urban et al., 1989). Once mobilized, DOC can influence aquatic ecosystem productivity, alter light regimes, and drive microbial activity, with cascading impacts on greenhouse gas

https://doi.org/10.5194/egusphere-2026-3284
Preprint. Discussion started: 19 June 2026

(GHG) fluxes and aquatic food webs (Creed et al., 2018; Solomon et al., 2015). Further, a portion of this exported DOC reaches marine environments, contributing to carbon cycling at coastal margins (Kazmiruk et al., 2021). Though studies are limited, DOC is a potential additional source of CO_2 and CH_4 emissions through downstream mineralization (Aho & Raymond, 2019; Dinsmore et al., 2010), and in some studies DOC export, if accounted for, can switch peatlands from long term carbon sinks to sources (He et al., Submitted), particularly in disturbed landscapes (Roulet et al., 2007; Wallin et al., 2013).

Hydrological regime and connectivity are increasingly recognized as primary controls on both the production and export of DOC from peatland systems (Hribljan et al., 2014; Prijac et al., 2023; Strack et al., 2008). Near the surface (i.e., the variably saturated acrotelm (Ingram, 1978)), deep water tables expose peat to oxic conditions, stimulating microbial decomposition and enhancing DOC production (Blodau et al., 2007; Waddington et al., 2015). Upon rewetting, this accumulated DOC may be flushed laterally, generating concentrated pulses downgradient and into receiving waters (Prijac et al., 2023; Ritson et al., 2017; Tiwari et al., 2022). At greater depths, in the perennially saturated, anoxic catotelm (*sensu* Ingram, 1978), microbial activity is more constrained (Basiliko et al., 2007; Wilson et al., 2016) and flowpaths are often poorly connected due to low conductivity peat dominated by small pores and disconnected pore networks (Rezanezhad et al., 2016a). In this zone, slow transit times can promote long-term DOC preservation and thus accumulation (Wilson et al., 2016), particularly if fresh organic matter is transported downward from the active near-surface layers (Zarov et al., 2023). These vertically stratified dynamics underscore the layered influence of hydrological conditions on DOC cycling.

The dynamic nature of DOC production and export aligns conceptually with the “fill-and-spill” framework (Spence & Woo, 2003), which has been widely used to describe intermittent hydrological connectivity in wetland systems. In this framework, lateral water movement between wetland units and towards downgradient features is constrained by internal storage thresholds that must be exceeded before connectivity is established, with higher storage states enabling the expansion of contributing areas beyond individual wetlands to include larger portions of the watershed (Branfireun & Roulet, 1998; Quinton & Roulet, 1998). These shifts in connectivity not only reorganize flowpaths across the landscape but also influence the transport and transformation of solutes along those pathways (Devito et al., 2017). In peatland systems, these thresholds are strongly controlled by the exponential decrease in peat transmissivity with depth (McCarter & Price, 2017), such that relatively small changes in water table position can trigger abrupt transitions from hydraulically disconnected conditions to active lateral flow and widespread hydrological connectivity. Under a classical fill-and-spill conceptual framework, connectivity across peatland landscapes is expected to increase primarily when water tables rise into the near surface (Spence & Woo, 2003), typically within the top ~5–30 cm, depending on peatland type and landscape position (Balliston & Price, 2022; Connon et al., 2015; Goodbrand et al., 2019; McCarter & Price, 2017).

While the fill-and-spill concept has not been explicitly applied to DOC movement, the episodic nature of DOC export—particularly during snowmelt and storm events (e.g., Clark et al., 2007; Dawson et al., 2008; Rosset et al., 2020)—suggests that similar threshold-mediated mechanisms may influence DOC mobilization along the flowpath, especially from near-surface soil layers. Studies have observed that rainfall-driven increases in water table depth and

https://doi.org/10.5194/egusphere-2026-3284
Preprint. Discussion started: 19 June 2026

hydrological connectivity coincide with DOC export pulses, highlighting the coupling between peatland hydrology and carbon transport (Dawson et al., 2008; Prijac et al., 2023; Strack et al., 2008). However, these patterns are further shaped by vertical structure and internal heterogeneity, including the presence of preferential flowpaths, both near the surface where they may occur as localized depressions (Balliston et al., 2018; McCarter & Price, 2017), and at depth, the latter of which may bypass surface thresholds entirely and transmit DOC rapidly from deeper or hydrologically disconnected zones (Billett et al., 2012; Carey & Woo, 2000; Holden et al., 2012; Holden & Burt, 2002).

Despite its importance to northern ecosystems and regional carbon budgets, the hydrological mechanisms governing DOC mobilization and delivery along the peatland–surface water continuum remain incompletely understood. Most existing studies emphasize relationships between DOC export and bulk hydrological metrics such as stream discharge and water table position, whereas far less is known about how DOC is mobilized and transmitted along flowpaths from catchment headwaters to downgradient surface waters. The relative roles of near-surface versus deeper flowpaths, the prevalence of preferential pathways and the conditions under which they become activated, and the extent to which DOC export is sustained outside classical fill-and-spill connectivity states remain poorly constrained. Although evidence from blanket peatlands in the UK shows that preferential flowpaths can act as efficient conduits for rapid and disproportionate carbon transport (e.g., Billett et al., 2012; Holden et al., 2012; Holden & Burt, 2002; Smart et al., 2013), the extent to which similar mechanisms operate in peatland systems with contrasting structure, hydrological regimes, and landscape organization, such as those across the Canadian boreal and subarctic, remains largely unknown. Mechanistic understanding of DOC delivery to lakes, where groundwater discharge and shoreline heterogeneity can dominate hydrologic exchange, also lags far behind that for stream-receiving peatlands. Resolving how catchment structure, including slope, peat stratigraphy, wetland type, flowpath geometry, and wetland composition controls DOC mobilization is therefore essential for predicting carbon export under current and future hydroclimatic conditions.

Our study focuses on a peatland-dominated headwater watershed situated at the southern ecotonal boundary between the Precambrian Shield and the Hudson Plains (i.e., the Hudson and James Bay Lowlands) in northeastern Ontario, Canada. The Hudson Plains ecozone contains an estimated ~30 Pg of organic carbon, making it the third-largest contiguous peatland complex globally and one of the most significant long-term terrestrial carbon reservoirs (Li et al., 2025a; Packalen et al., 2014). Yet the southern headwaters remain poorly characterized, even though these transitional zones serve as critical points of hydrological and biogeochemical initiation. Here, deep peat accumulation occurs in landscapes marked by greater topographic relief, heterogeneous mineral substrates, and mixed wetland types (Finkelstein et al., 2023; Sothe et al., 2022). Understanding how intact peatland systems in these headwater settings store and release carbon is critical for anticipating downstream impacts and informing evidence-based decisions, particularly given the intensifying climate change and development pressures in the area (Harris et al., 2022).

Through this study, we aimed to advance mechanistic understanding linking hydrological connectivity and DOC cycling in northern peatland-dominated watersheds and provide insight into the landscape-scale processes driving

https://doi.org/10.5194/egusphere-2026-3284
Preprint. Discussion started: 19 June 2026

DOC flux to boreal lakes. In this context, our objectives were to: (1) Characterize how peatland structure and landscape setting constrain lateral flowpaths from catchment headwaters to boreal lakes across a range of hydrological conditions; (2) Identify the spatial and temporal patterns of peatland-to-lake connectivity and determine the conditions under which flowpaths become hydraulically active; and (3) Quantify the magnitude, direction, and variability of DOC transport along these flowpaths, and evaluate how DOC dynamics vary across space and time.

1.1 Study Region and Site Description

The study site is situated within the North French River (NFR) watershed (Cree: Kâpâyâw Sîpiy), a remote and relatively pristine subwatershed of the Moose River on the traditional territory of the Moose Cree First Nation (MCFN) in northern Ontario, Canada (Figure 1a). The NFR spans two distinct ecozones: it originates in the transitional portion of Precambrian Shield (sometimes historically referred to as the "Clay Belt" (Liu, 1990)) and flows northeastward into the Hudson Plains, eventually joining the Moose River near James Bay. These zones differ markedly in topography and depositional history. The transitional area of the Shield features undulating terrain and heterogeneous glaciolacustrine sediments (Saurette et al., 2018) whereas the Plains are exceptionally flat and underlain by thick, relatively uniform marine deposits (Dredge & Dyke, 2020); in both regions, where these deposits are fine-grained they can act as aquitards, limiting downward water seepage and promoting peat accumulation.

Wetlands cover over 75% of the NFR watershed, with a higher incidence of swamp cover in the Shield headwaters relative to the Plains (OMNRF, 2014). While peat depths in the Plains are relatively well characterized, data for the transitional Shield remain sparse (Ekstrom et al., 2007; Li et al., 2025). To address this knowledge gap, the study site was purposefully located in the transitional Shield, with input from MCFN Land Guardians to identify areas of likely peat accumulation.

The study focuses on Tomorrow Lake and its 2.3 km² catchment, (Figure 1b; 49° 54' 50.2"N, 80° 41' 42.0"W) located centrally within the Shield ecozone (Figure 1a). The Yesterday River (Cree: Wawagigamau), a tributary of the NFR, flows through the lake from south to north. This site holds cultural and traditional significance to the Moose Cree First Nation and encompasses the diverse wetland and surface water features characteristic of the surrounding landscape. Land cover classification identifies the catchment as approximately 85% wetland, dominated by coniferous swamp, with localized areas of treed bog and fen (Figure A1a). The remaining 15% is classified as forested non-wetland, though the accuracy of this classification is likely limited due to dense canopy cover over low-lying terrain (Li et al., 2020).

https://doi.org/10.5194/egusphere-2026-3284
Preprint. Discussion started: 19 June 2026

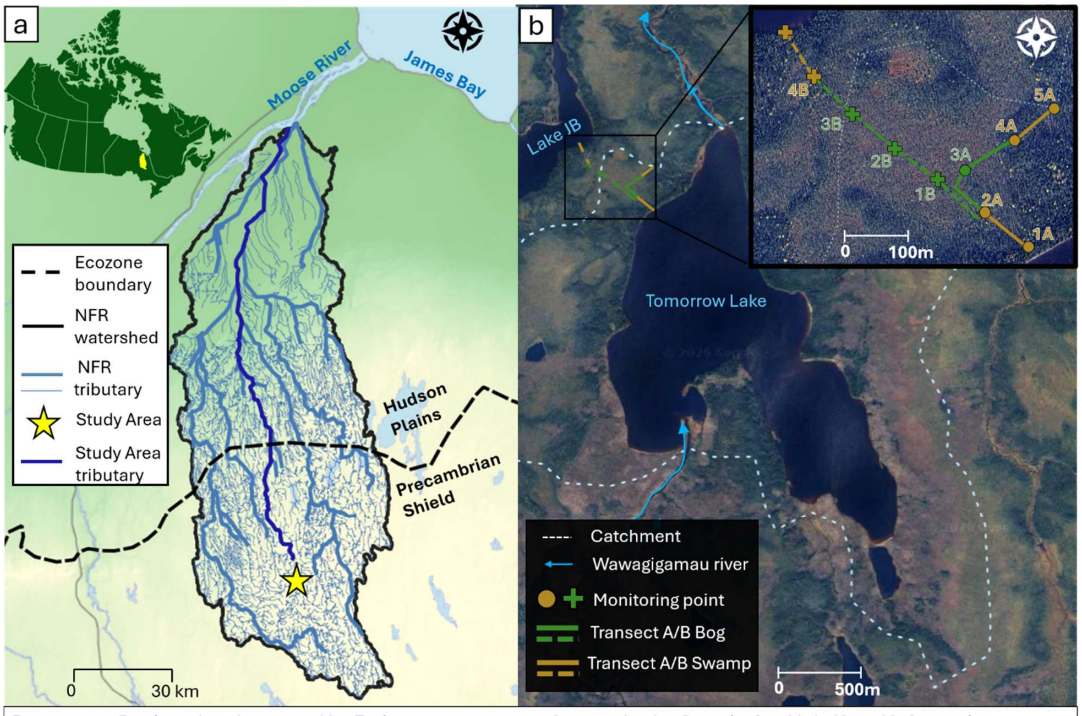

Basemaps: Designed and powered by Esri; watercourses and watersheds: Ontario GeoHub / Land Information Ontario, licensed under the Open Government Licence – Ontario.

Figure 1. a) Tributaries (blue lines) of the North French River watershed (solid black outline) located in the traditional territory of Moose Cree First Nation. The study site (yellow star) is located in the Precambrian Shield portion of the watershed and is centered on b) Tomorrow Lake and its 2.3 km² catchment (dashed white line). Research transects A and B (yellow lines) are located at the northwest end of the lake.

2 Methods

2.1 Transect Selection and Instrumentation

In June 2024, a 400 m transect (Transect A; Figure 1b) was established in the northwest corner of the Tomorrow Lake catchment, beginning at the inferred catchment elevation high based on available digital elevation model (DEM) data (NRCan, 2000; Figure A1b), and following the topographic gradient downslope to the lake. Five equally spaced monitoring nests (1A to 5A) were installed along the transect (Figure 1b). Each nest comprised a set of 30 cm screened 1-inch (2.54 cm) diameter PVC piezometers positioned with the screen centred at depths of 75, 100, 150, and 200 cm below ground surface (bgs) where feasible, or to refusal where mineral substrates impeded installation. Each nest was also equipped with a fully screened 1.25-inch (3.18 cm) diameter well (installed to refusal) and two porewater samplers of 10 cm screen length centred at 30 and 50 cm bgs.

Initial wetland "units" were delineated during site visits using Far North Land Cover classifications (OMNRF, 2014; Figure A1a) (e.g., treed bog, treed coniferous, coniferous swamp), and refined in the field according to the Canadian Wetland Classification System (National Wetlands Working Group, 1997). The first ~100 m from the lakeshore

https://doi.org/10.5194/egusphere-2026-3284
Preprint. Discussion started: 19 June 2026

(nests 1A and 2A; Figure 1b) was classified as an organic lagg swamp (Swamp 1; Figure A2a) located above lake level and dominated by a dense overstory of *Picea mariana*, with an understory of *Gaultheria hispidula, Kalmia angustifolia, Ledum groenlandicum* and *Vaccinium uliginosum,* along with a mixed moss layer of *Sphagnum* and feathermoss species. At ~120 m, Swamp 1 transitioned into a treed domed bog (Bog 1; Figure A2a) characterized by stunted *P. mariana,* dense shrub cover *(V. uliginosum, L. groenlandicum,* and *Chamaedaphne calyculata),* and a continuous carpet of *Sphagnum* moss. The flowpath shifts ~90° midway through Bog 1 and continues northeast through nest 3A (Figure 1b), eventually grading into an organic mound swamp (Swamp 2; Figure A2a) that occupies the catchment's topographic high and exhibits vegetation similar to Swamp 1.

During field activities in 2024 it was observed that although the instrumented portion of Bog 1 lies downslope of Swamp 2, a secondary topographic high exists within Bog 1 west of nest 3A. To investigate the potential influence of this secondary flowpath on hydrological and biogeochemical processes, a second temporary transect (Transect B; Figure 1b) was installed in May 2025. Transect B extends northwest beyond this secondary rise (Bog 1B; Figure A2b), through a second organic lagg swamp (Swamp 3) and terminates at a small adjacent lake (Lake JB), which drains northeast outside the Tomorrow Lake catchment. Four multilevel samplers (screened at 50, 100, 150 and 200 cm) were installed at 100 m intervals along Transect B and removed in September 2025 to minimize disturbance.

To capture meteorological conditions, a weather station was installed at nest 3A in June 2024. Measurements included rainfall (52203-L RM Young Tipping Bucket Rain Gauge), air temperature, barometric pressure, wind speed and wind direction (METSENS500 weather sensor). Due to animal interference, the station was non-functional from October 2024 to June 2025; during this period, temperature and precipitation data were supplemented using records from the nearest Environment and Climate Change Canada (ECCC) climate station at Moosonee ~150 km north (Table A1). A snow depth gauge and a GardePro A3S trail camera were installed at 3A in September 2024 to record snow depth via time-lapse photos taken every six hours. Snow water equivalent (SWE) could not be calculated because snow density measurements were not collected.

2.2 Transect Subsurface Characterization

Peat depth and the underlying mineral substrate type (where encountered) were assessed at each nest during initial transect installation. Grain size analysis was determined using visual–textural classification based on particle size and tactile properties (e.g., cohesion, grittiness), following standard soil description methods.

To resolve fine-scale variations in surface elevation and slope, a relative elevation survey was conducted in May 2025 using a Smart Level (±1 cm accuracy). Measurements were collected at 1 m intervals from the lakeshore to nest 1A, and every 10 m thereafter along both transects, using a fixed reference point on the Tomorrow Lake shoreline as the site datum. Supplementary peat depth measurements were collected in August 2025 at each elevation point, although this was discontinued beyond 70 m from the shoreline due to equipment damage.

To support groundwater flowpath modelling, hydrophysical properties were characterized across Transect A. Saturated hydraulic conductivity (K_{sat}) was determined in 2025 at all piezometer locations, with each installation tested at least twice. Slug tests were performed by rapidly removing ≥20 cm of water and recording recovery using

https://doi.org/10.5194/egusphere-2026-3284
Preprint. Discussion started: 19 June 2026

Van Essen TD-Diver® pressure transducers. Tests were terminated once ≥90% recovery was observed. K_{sat} was then calculated using the Hvorslev (1951) hydrostatic time-lag method.

To better resolve the hydrologic properties of the upper peat profile, commonly considered the zone of greatest hydrophysical variability (e.g., Morris et al., 2022), six near-surface peat cores (25 cm depth, 10 cm diameter) were collected along the transect to represent the dominant ground cover types. Each core was sectioned into 5 cm increments and analyzed in the laboratory for K_{sat} using a constant-head Darcy permeameter. Total porosity was also determined for each slice to support flowpath modelling, under the assumption that porosity equaled water content at saturation. Porosity (θ_{sat}) was calculated using Eq. (1)

$$\theta_{sat} = n_t = \frac{(M_{sat} - M_{dry})}{V_t \rho_w} \quad (1)$$

where θ_{sat} is the saturated volumetric water content (-), n_t is total porosity (-), M_{sat} is the saturated core weight (g), M_{dry} is the dry core weight (g), V_t is the saturated core volume (cm^3) and ρ_w is the density of water (1 gcm^{-3}).

In the absence of instrumentation at the transect outlet, peat depth and mineral substrate type were assessed every 1 m from the lake shoreline to nest 1A. Due to marked heterogeneity in the underlying mineral sediments, 16 shallow mineral samples (5 cm deep, 2 cm diameter) were collected between the shoreline and 1A to better characterize conditions at the peat–lake interface. These samples were analyzed using the same laboratory protocols applied to the near-surface peat cores, ensuring consistency in estimates of outlet conductivity.

During transect installation in May 2024, a suspected groundwater spring with no apparent surface inflow was discovered approximately 5 m west of the Transect A outlet (Figure A3a). Thermal imaging using a handheld infrared camera (FLIR E5 Pro) confirmed cooler water temperatures at the site relative to surrounding surface waters (Figure A3b), supporting the interpretation of groundwater discharge. This groundwater spring was sampled during all monitoring events in 2024 and 2025. In 2024, flow was measured manually; in 2025, the spring was instrumented with a V-notch bucket weir (maximum capacity: 1 Ls^{-1}) and fitted with a HOBO U20L pressure transducer to log continuous flow from June to September 2025 (Figure A4).

2.3 Hydrological and Biogeochemical Monitoring

Hydrological monitoring and sampling were conducted in 1–2-week campaign-style intervals at Transect A in June, August, and September 2024, and at both Transects A and B in June and August 2025. At Transect A, each campaign included measurements of hydraulic head in all installed wells and piezometers. In addition, pressure transducers (Van Essen TD-Diver®) were deployed at nests 3A and 5A in June 2024, and subsequently at nests 1A, 2A, and 4A in August 2024. These transducers recorded water table elevations at 30-minute intervals, with values barometrically corrected using a Van Essen Baro-Diver® and referenced to cm below ground surface (bgs) using manual measurements. Given the temporary nature of Transect B and the goal of minimizing site disturbance, no permanent wells or piezometers were installed there.

In both 2024 and 2025, water samples were collected from all piezometers and porewater sippers at Transect A, as well as from Tomorrow Lake and opportunistic surface water points along the transect. In 2025, additional samples

https://doi.org/10.5194/egusphere-2026-3284
Preprint. Discussion started: 19 June 2026

were collected from all multilevel samplers installed along Transect B. Field variables—water temperature (T; °C), specific conductance (SPC; µS cm^{-1}), and pH (–)—were measured in situ using a YSI EXO2 multiparameter sonde. Samples were then transferred to 40 mL amber glass vials, field-filtered at camp accommodations using 0.45 µm glass syringe filters, and transferred into clean secondary amber glass vials. Samples were stored on ice and in the dark until analysis. Within three days of filtration, all samples were acidified and subsequently analyzed for dissolved organic carbon (DOC) concentration within one week. DOC analysis was conducted using a Shimadzu TOC-LCPH/CPN Analyzer at the University of Waterloo Ecohydrology Laboratory (2024) and the Great Lakes Watershed Ecology Research Laboratory (2025), with a MDL of <0.2 mgL^{-1}.

2.4 Flowpath Modelling and Spatial Analysis

2.4.1 Subsurface Flowpath Modelling and Travel Time Estimation

Subsurface flowpath geometry and associated travel times were modelled using the USGS TopoDrive software, parameterized with measured hydrophysical properties, water tables, and surface and subsurface topography. Because TopoDrive defines the upper boundary of the model domain as the water table surface, the shallowest recorded water tables were used to capture the full range of field conditions. The model was used to estimate relative flowpath geometry and travel times under representative hydrological conditions and was not intended to reproduce transient field dynamics or absolute fluxes. The model domain was parameterized using five distinct areas representing binned, geometrically averaged saturated hydraulic conductivity (K_{sat}) and porosity values derived from field measurements and collected samples (Table A2; Figure A5-A6). An order-of-magnitude hydraulic conductivity anisotropy was applied within near-surface peat, consistent with values commonly reported for fibric to mesic peat layers (Beckwith et al., 2003), whereas deeper peat layers and underlying mineral sediments were treated as isotropic because of limited evidence for preferential hydraulic orientation at depth. Porosity values of 0.8 for deep peat, based on literature values (Letts et al., 2000), and 0.35 for the underlying till, based on 16 transect samples, were applied where direct field measurements were unavailable. These porosity estimates primarily influence relative, rather than absolute, travel time estimates. To better reflect microtopographic variation encountered in the field, an acrotelm thickness of 30 cm was applied to the model using an average of the properties obtained in the 25 cm cores.

Once parameterized, flowpaths were initiated across the model domain to estimate subsurface travel times to the outlet (Figure A6b). Although TopoDrive implements a steady-state representation of subsurface flow, two-dimensional steady-state models have been shown to be effective in peatland-dominated systems for evaluating flow configurations, hydraulic gradients, and connectivity (Price et al., 2023). Model-derived flowpath geometries were evaluated against manually measured hydraulic head data collected during the five primary monitoring events.

2.4.2 Spatial Interpolation of Hydraulic and Biogeochemical Data

Hydraulic head and biogeochemical variables, including T, pH, SPC, and DOC, were spatially interpolated across the transect for each sampling event using Surfer (Golden Software, LLC, Golden, Colorado, USA) to generate two-dimensional contour surfaces. Initial interpolations were produced using both inverse distance weighting (IDW) and kriging to assess sensitivity to interpolation method. Interpolated contours were then refined to improve consistency

https://doi.org/10.5194/egusphere-2026-3284
Preprint. Discussion started: 19 June 2026

with (i) observed hydraulic gradients, (ii) manually measured water levels, and (iii) known hydrophysical stratigraphy. Model-derived flowpath geometries were used as an independent line of evidence to aid contour interpretation. Adjustments generally emphasized lateral continuity over vertical continuity, consistent with the anisotropic hydraulic structure characteristic of peatland systems. In addition to event-specific contour maps, mean contour surfaces and corresponding standard deviation maps were calculated across the five monitoring events to characterize average conditions across the transect.

3 Results

3.1 Peatland structure and landscape setting

Transect characterization revealed pronounced spatial heterogeneity in topography and mineral substrate composition, establishing a complex structural framework within which these wetland units have developed. Surface slope varied systematically with landscape position, with relatively flat conditions at topographic highs (e.g., Swamp 2 and the elevated region within Bog 1; 0.1–0.2 cm m^{-1}), transitioning to steeper gradients toward downgradient lake margins (Table 1; Figures A1b, A2). The steepest slopes occurred within lagg zones at the lake interfaces, exceeding 7 cm m^{-1}, whereas intermediate slopes (0.3–0.7 cm m^{-1}) were observed along the flanks of Bog 1. Substrate composition was primarily silty clay with locally enriched lenses of sand and gravel by nests 4A and 5A and at the Transect A outlet.

Peat depth varied independently of both topography and landscape position, reflecting strong subsurface heterogeneity. The first hotspot of very deep peat (>400 cm) occurred at the crest of Bog 1 along Transect B, whereas the topographic high in Swamp 2 along Transect A was associated with comparatively shallow peat (50 - 75 cm; Table 1, Figure A2a). At the lake interface along Transect A, peat thickness was minimal (<10 cm), but increased rapidly inland to a second hotspot of very deep peat within 50 m. In contrast, peat remained substantially thicker along Transect B to the Lake JB shoreline (>40 cm) but was less deep in Swamp 3 than in Swamp 1(Table, Figure A2b). Notably, locations with shallow peat coincided with underlying mineral sediments enriched in sand and gravel. These coarser-grained sediments are consistent with a semi-confining or “leaky aquitard,” that may permit greater vertical exchange between peat and underlying mineral layers relative to finer-grained substrates.

3.2 Hydrological controls on water table dynamics and hydraulic gradients

Hydrological conditions differed markedly between the two monitoring years. In 2024, conditions were substantially warmer and drier than the 1991–2020 climate normals (Table A1), with a precipitation deficit of ~180 mm, nearly half of which occurred in August and September. In contrast, 2025 was cooler and wetter, with precipitation during late June alone exceeding that recorded over the entire June–September period in 2024 (Table A1; Figure 2). Despite these variations in water availability, measured lateral hydraulic gradients remained consistently aligned with surface slope throughout the monitoring period, indicating stable downslope flow (Table 1). Vertical hydraulic gradients were more complex, with greater temporal and spatial variability (Tables 1, A3). Gradients were predominantly downward under Bog 1; however, both upward and downward gradients were observed in Swamps 1

https://doi.org/10.5194/egusphere-2026-3284
Preprint. Discussion started: 19 June 2026

and 2 and mid-profile reversals were common at most nests and monitoring events (Figure A7), further indicating layered or transient flow conditions within the peat profile.

Measured water table depth varied systematically with water availability, landscape position, and wetland type. Across the non-frozen period (May-October), water tables generally deepened from spring to summer and with increasing elevation (Table 1; Figure 2). In Swamp 1, water table remained within 30 cm of the surface for the majority (> 90%) of the monitoring period, whereas in Bog 1 and Swamp 2, near-surface saturation was limited to snowmelt and following major rainfall events (~35% and 0-20% of the study period, respectively; Figure 2). The deepest water tables were observed at nest 5A in Swamp 2, where water level dropped below the peat profile and into the underlying mineral sediments during the 2024 drought. Although water table was not directly measured along Transect B, frequent drying of shallow samplers (50 cm bgs) indicates limited near-surface saturation during the 2025 monitoring period.

Table 1. Peat depths and hydrological variables (water table depth vertical gradients, and lateral gradients) where measured Transects A and B). Peat depths are reported in cm, water table depths are in cm bgs, and surface slope and hydraulic gradients are in cm m^{-1}. Values were calculated for the non-frozen season (May-October). Positive vertical gradients indicate upwards flow, and positive lateral gradients indicate downslope flow in decreasing numerical order (i.e. 5-4)

	Nest	Peat Depth	Surface Slope	WTD avg ±stdev		Vertical Grad avg ±stdev	Lateral Grad avg ±stdev
				2024	2025		
Tomorrow Lake Interface	-	<5	7.2	--	--	--	--
Swamp 1	**1A**	95	2.7	28 ± 10	24 ± 4	-5.3 ± 9.7	2 ± 0.2
	2A	150	0.70	26 ± 7	24 ± 4	1.8 ± 2.4	0.7 ± 0.02
Bog 1	**3A**	400	0.46	34 ± 4	32 ± 3	-1.7± 1.8	0.4 ± 0.05
Swamp 2	**4A**	50	0.28	42 ± 12	35 ± 7	14.2± 13.8	0.2 ± 0.08
	5A	75	-0.18	54 ± 5	51 ± 4	-4.5± 21.0	-0.03 ± 0.008
Bog 1	**1B**	>400	0.64	--	--	--	--
	2B	327	0.080	--	--	--	--
	3B	130	-0.28	--	--	--	--
Swamp 3	**4B**	292	-0.91	--	--	--	--
Lake JB Interface	-	57	-2.2	--	--	--	--

https://doi.org/10.5194/egusphere-2026-3284
Preprint. Discussion started: 19 June 2026

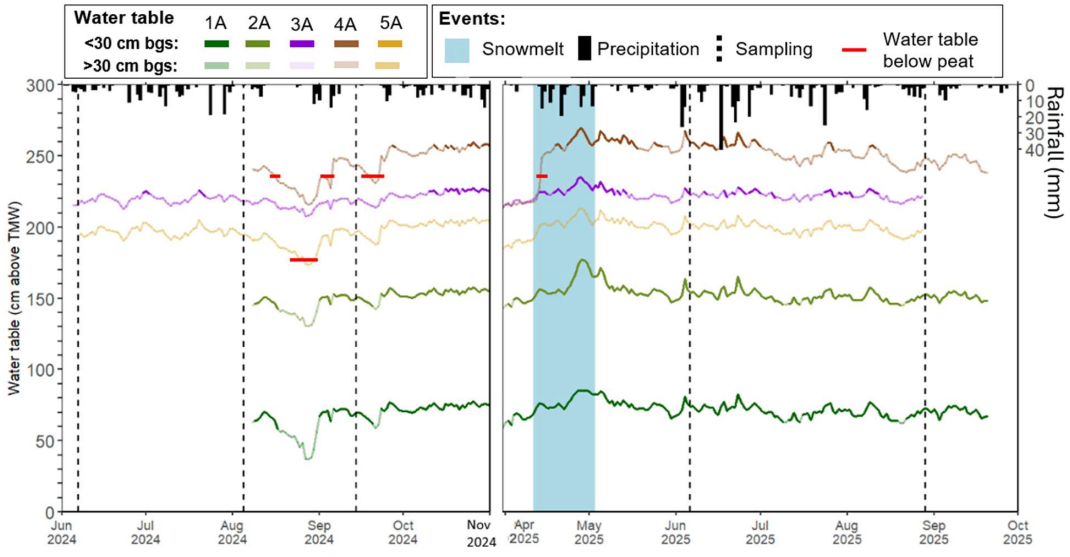

Figure 2. Continuous water table elevations (cm above shoreline) along Transect A (lines) and select meteorological processes including daily precipitation (black boxes) and spring melt (blue shaded area). Sampling events are marked by dashed vertical lines.

3.2 Flowpath geometry and hydrological connectivity

Subsurface characterization revealed strong vertical and lateral variability in soil properties. Measured lateral saturated hydraulic conductivity (K_{sat}) across Transect A varied by over five orders of magnitude within the peat profile, and over seven orders of magnitude in the underlying mineral sediments (Figures 3, A5; Table A2). The highest K_{sat} values (~9 x 10^{-3} m s^{-1}) were observed in near-surface peat, with K_{sat} generally decreasing with depth. However, a localized zone of elevated K_{sat} was identified in the deepest peat beneath nests 2A and 3A (Figure 3). Mineral K_{sat} values (10^{-8} to 10^{-6} m s^{-1}) were consistent with glacial till to silty sand (Freeze & Cherry, 1979), with higher conductivity observed beneath Swamp 2 and near the transect outlet.

Model-derived subsurface flowpaths (Figures 3, A6) aligned closely with interpolated hydraulic head contours derived from all five monitoring campaigns (Figure A7), indicating stable flowpath geometry under varying hydrological conditions. From the topographic high in Swamp 2 at nest 4A, flowpaths descended vertically before diverging laterally toward 5A and Tomorrow Lake, broadly following surface slope. A distinct inflection in flow direction occurred between nests 2A and 3A across multiple depths (Figures 3, A7), separating flow into shallow and deep domains. Above ~75 cm bgs, flowpaths remained predominantly lateral and downgradient toward the outlet. Below this depth, flow was directed vertically downward beneath 3A, then laterally along the organic–mineral interface before turning upward beneath 1A and re-emerging closer to the surface, thereby bypassing the near-surface zone.

Under the shallowest water table conditions (Figure A6), minimum transit times to the outlet from Swamp 1, Bog 1 and Swamp 2 occurred the near surface acrotelm and were on the order of 10, 100 and 500 days, respectively. When

https://doi.org/10.5194/egusphere-2026-3284
Preprint. Discussion started: 19 June 2026

constrained to the average water table position across the monitoring period (Figure 3), desaturation of near-surface peat within Bog 1 and Swamp 2 restricted flow to the lower conductivity catotelm with seepage velocities < 0.5 m day^{-1}, yielding transit times to the outlet on the order of decades to centuries. Flow remained rapid in Swamp 1 (1-10 m day^{-1}) due to its close proximity to the outlet and acrotelm saturation.

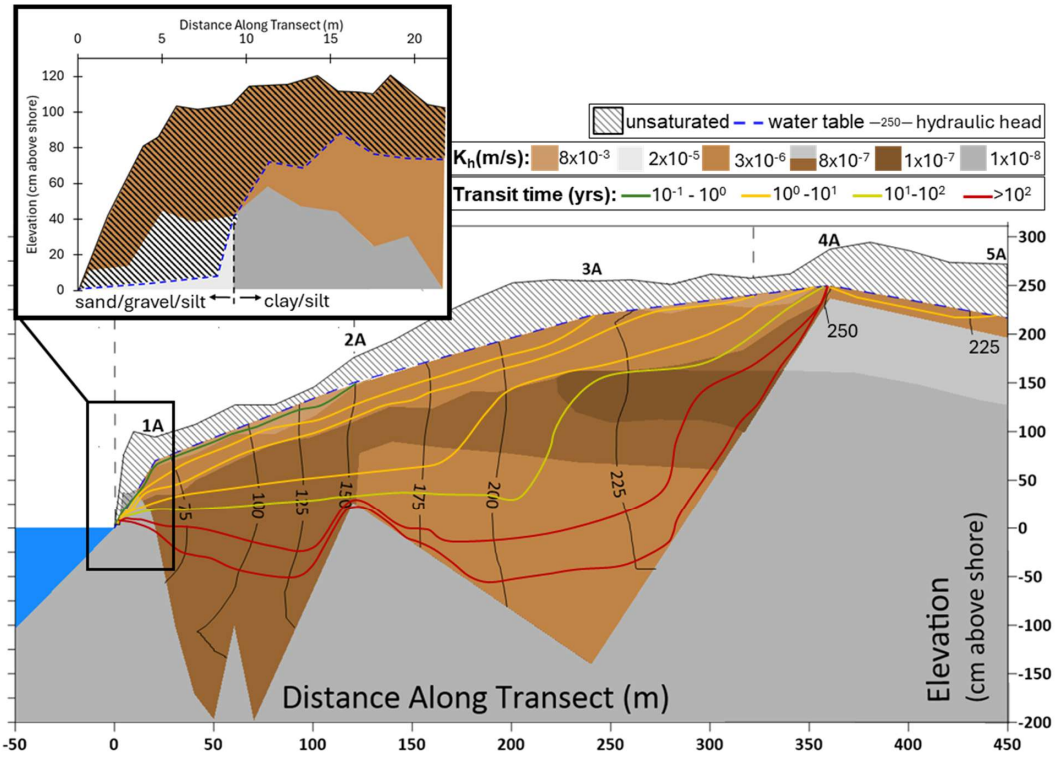

Figure 3. Finalized transect peat (brown) and mineral (grey) stratigraphy delineated by spatially similar and averaged representative lateral K_{sat} values (darker shades indicate lower K_{sat}). Modelled flowpaths were generated using Topodrive and colour coded by transit time from flowpath origin to transect outlet (Figures A6-A7). The dashed line reflects the average water table depth across the study period.

3.2.1 Groundwater Discharge at the Lake Margin

Detailed field characterization of the transect outlet from nest 1A to the shoreline revealed a notable drop in the water table ~10 m from the lake, which coincided with the tapering of peat to 0 cm and shift from silt/clay to sand and gravel (Figure 3 insert). Samples from this transitional mineral layer yielded a median K_{sat} of 2 x 10^{-5} m s^{-1} (Figure A8) consistent with the upper range reported for unconsolidated glacial materials (Earle, 2015). Along the shoreline, this mineral interface occurred intermittently alongside zones of direct peat–water contact, indicating spatial variability in discharge conditions.

Discharge from the groundwater spring instrumented in 2025 was highly variable and characterized by event-driven, flashy dynamics (Figure 4). The majority (>90% of) total discharge occurred during short-duration, high-flow events (> 0.5 L s^{-1}; blue bars in Figure), typically associated with rainfall events ≥ 10 mm day^{-1} The largest event in late June 2025 (78 mm of rainfall total) accounted for ~40% of the cumulative discharge over the entire instrumented

https://doi.org/10.5194/egusphere-2026-3284
Preprint. Discussion started: 19 June 2026

period. Low flow periods (<0.01 L s^{-1}; red bars in Figure) contributed minimal discharge despite comprising 25% of the time. Response times to rainfall varied seasonally, with rapid increases in discharge during early summer and longer response lags later in the season, indicating evolving hydrological connectivity at the outlet.

Although measured water table depths at all five monitoring wells were significantly correlated with groundwater spring discharge ($p<0.01$, Figure A9), substantial scatter and overlap between low- and high-flow conditions were observed. This variability reflects seasonal shifts in the relationship between water table position and discharge, with water tables associated with high flow conditions deepening over time at several nests (Figure A10). Together, these results indicate that discharge was not solely controlled by water table position but was strongly influenced by event-driven connectivity and subsurface flow routing.

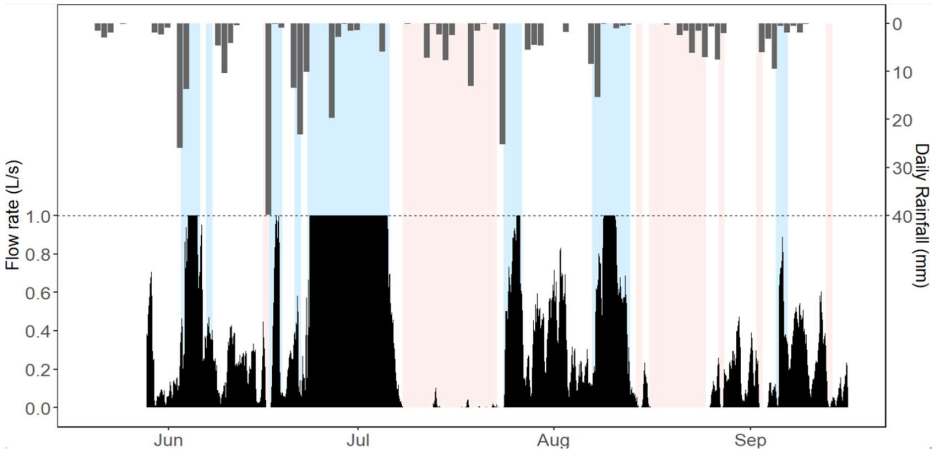

Figure 4. Groundwater spring flow rates measured continuously from June to September 2025 at the transect outlet. Periods of no or negligible flow (<0.01 L s^{-1}) are indicated by red shading while periods of high flow (0.5 L s^{-1}) are indicated by blue shading. Daily precipitation totals are indicated as grey bars. The overtopping threshold of 1 L s^{-1} is denoted by the horizontal dashed line; calculated flow rates above this value were conservatively set to 1 L s^{-1} to avoid flow overestimation.

3.3 Biogeochemical Patterns and DOC Export Along the Peatland–Lake Continuum

Interpolated contour surfaces of pH, specific conductance (SPC), and porewater temperature (T) along Transect A showed strong temporal consistency across monitoring events (Figures A11-A13), supporting their synthesis into composite average maps (Figure 5). Vertically, SPC and pH generally increased, while T decreased with depth from the near-surface peat to the underlying mineral substrate. Laterally, distinct zones of low pH and elevated T were observed at depth between Bog 1 and Swamp 1 (nests 3A to 2A), as well as the downgradient section of Swamp 2 (nest 5A; Figure 5b, c).

Observations from Transect B exhibited similar vertical trends in SPC and pH, revealing a similar depth-dependent geochemical signature across the site (Figure A14). However, temperature patterns varied seasonally, with a warmer subsurface observed June 2025 and the more typical decrease in temperature with depth by August (Figure A14e, f). The low-pH, low-SPC plume observed between 2A and 3A (Figure 1a,b) extended into this section of the bog (Figure A14a-d); even the deepest peat layers here remained acidic (pH < 4.4).

https://doi.org/10.5194/egusphere-2026-3284
Preprint. Discussion started: 19 June 2026

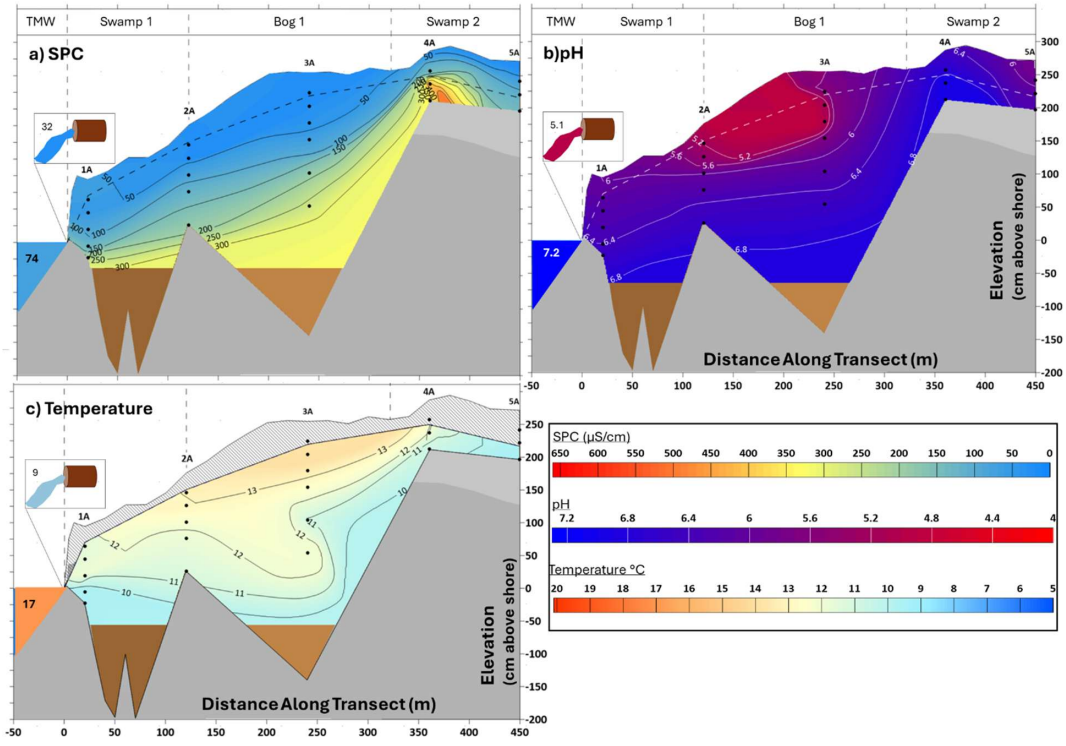

Figure 5. Temporally averaged Transect A contours depicting a) specific conductance (SPC; µS cm^{-1}) b) pH (-) and c) temperature, over the June 2024 to August 2025 monitoring period. Conditions at the groundwater spring are shown in the inset pipe image in each panel.

Measured DOC concentrations varied substantially across both space and time (Figure 6). Along Transect A, DOC generally increased from spring to summer in both years, with the development of a persistent, DOC-rich subsurface plume beneath Bog 1. This plume expanded laterally downgradient toward Swamp 1 between June and September 2024 (Figure 6 a-c) and remained detectable into the following year, although by August 2025 DOC accumulation was mostly confined to the upper 75 cm (Figure 6d-e). Along Transect B, DOC exhibited distinct but complementary patterns (Figure 6f-g), with high concentrations (>200 mg L^{-1}) observed at depth downgradient of the bog dome in June 2025. By August, DOC concentrations were lower and more spatially diffuse, extending further downgradient, consistent with subsurface transport at depth. Together, these patterns indicate that DOC production and transport were strongly structured by depth and flowpath organization, with significant storage and movement occurring below the near-surface zone.

3.4.1 Outlet and Surface Water Biogeochemistry

Due to the absence of direct measurements at the shoreline and the heterogeneous nature of the lake margin, a harmonic mean of biogeochemical variables across the 1A peat profile was used as a proxy for subsurface inputs to Tomorrow Lake (Table 2, A4). This proxy closely matched transect-wide average conditions across monitoring

https://doi.org/10.5194/egusphere-2026-3284
Preprint. Discussion started: 19 June 2026

events, with the exception of slightly elevated DOC concentrations in September 2024 and lower concentrations during the following spring.

Groundwater spring pH, SPC and T values were consistently low and DOC concentrations remained high (Table 2); pH, SPC, and DOC most closely resembled values observed at the 30–50 cm depths within the low-pH plume identified between Bog 1 and Swamp 1 (Figures 5-6), while similar water temperatures were only observed in peat 100 –200 cm bgs across the transect often in contact with mineral substrate. Notably, the increase in deep peat DOC concentrations observed in Transect A during September 2024 coincided with the cessation of groundwater spring flow, whereas during periods of active discharge, DOC peaks were largely confined to the upper ~75 cm of the peat profile (Figure 6). Together, these patterns suggest shifts in the depth of subsurface sources contributing DOC to the outlet across sampling periods.

Table 2. Transect-wide and outlet-average values both within the soil and at the groundwater spring at each monitoring event (DOC only), and over the entire study period (DOC, pH, SPC, and T).

		Transect A Average	Outlet (1A Peat)	Outlet (Groundwater Spring)
Jun-24	DOC (mg L^{-1})	19	18	33
Aug-24	DOC (mg L^{-1})	27	27	39
Sep-24	DOC (mg L^{-1})	48	54	DRY
Jun-25	DOC (mg L^{-1})	23	18	24
Aug-25	DOC (mg L^{-1})	36	31	57
Average	pH	6.2	6.3	5.1
	SPC (µS cm^{-1})	130	148	32
	T (°C)	11.0	10.2	9.0
	DOC (mg L^{-1})	26	27	38

https://doi.org/10.5194/egusphere-2026-3284
Preprint. Discussion started: 19 June 2026

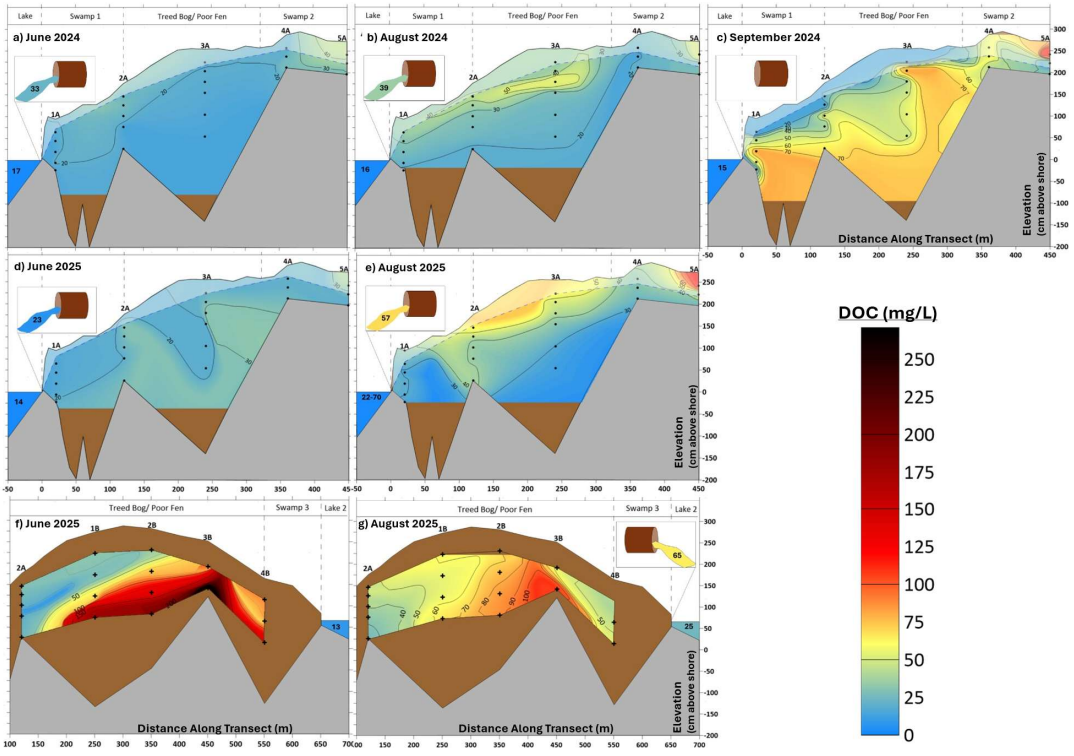

Figure 6. Transect A (a-e) and B (f-g) DOC (mg L^{-1}) contours measured during June, August and September 2024 (a-c) and June and August 2025 (d-g).

4.0 Discussion

4.1 Landscape structure controls peatland development and flowpath geometry

The stability and persistent alignment of lateral hydraulic gradients with surface topography (Table 1), and the nearly identical hydraulic head contours across all monitoring events (Figure A7), indicate that flowpath geometry is primarily structurally controlled rather than driven by transient variations in water availability. This contrasts with other peatland-dominated systems, where lateral flow may reverse between peatland units (Devito et al., 1997; Balliston & Price, 2022), adjacent mineral uplands (Elmes et al., 2021), or surface water features (Howie & van Meerveld, 2016; Langlois et al., 2015), acting as an important mechanism for redistributing saturation excess or retaining water during dry periods.

Flowpath geometry in this catchment is nonetheless complex, because transitions in elevation and land cover occur over short distances (Figures 1, A1), and similar landscape positions can support fundamentally different wetland morphologies (Figures 3, A2). This is illustrated by the two transect highs, Swamp 2 and Bog 1, which differ markedly in vegetation cover, peat thickness, and subsurface hydraulic properties (e.g., K_{sat}) despite occupying similar landscape positions (Table 1, Figures 3, A2). As in other boreal peatlands, this spatial heterogeneity likely originated from the morphology and composition of the underlying mineral substrate (Glaser et al., 2004a; Graniero

https://doi.org/10.5194/egusphere-2026-3284
Preprint. Discussion started: 19 June 2026

& Price, 1999), over which variable peat deposits have developed and now impose additional constraints on water movement.

Many of the structural contrasts most relevant to flowpath development are not readily apparent from surface datasets alone. For example, the dome of Bog 1 (3A to 1B) is not resolved in the available digital elevation model (Figure A1b), and its extent is substantially underestimated in the Far North Land Cover product (Figure A1a). Likewise, although the swamp units are somewhat better represented topographically, common land cover products do not distinguish between mineral and organic swamps (Hird et al., 2017; Kou et al., 2022). This distinction is especially important for Swamps 1 and 3 where peat depths exceeded 300 cm (Table 1; Figure A2), among the deepest 1% of deposits reported for the region (Davies et al., 2022; Li et al., 2025a). As a result, organic swamp systems may remain underrepresented in broader inventories (DeLancey et al., 2019; Webster et al., 2018), despite increasing recognition that swamp forests can store large carbon stocks (Davidson et al., 2022; Schmidt et al., 2025) and make significant hydrological contributions within boreal wetland networks (Devito et al., 2017).

Importantly, this structural variability is not simply a mapping challenge. Accurate characterization of subsurface structure and flowpath geometry is fundamental to understanding hydrological dynamics in other topographically complex wetland catchments, including those elsewhere in the Precambrian Shield (Devito et al., 2005) and across the boreal region (Lambert et al., 2022; Laudon et al., 2016), and to representing those dynamics realistically in hydrological models (e.g., Werner et al., 2021). Together, these observations highlight the continued importance of field investigation and ground-truthing alongside remote characterization. Geophysical approaches, including ground-penetrating radar, have proven effective for identifying such features (Holden et al., 2002; Moore et al., 2024) and represent a valuable direction for future work.

4.2 Water availability and storage regulation control the activation of structurally defined flowpaths

Measured hydraulic conductivity profiles across the transect (Figure 3) broadly followed the expected structure necessary for threshold-based connectivity, with an exponential decrease in K_{sat} from the near surface to the catotelm (e.g., Hoag & Price, 1995; Ingram, 1978; McCarter et al., 2017). However, residence of the water table within this transmissive near-surface zone varied substantially among landscape units (Figure 2), partitioning the catchment into functionally distinct hydrological domains. This pattern is consistent with broader observations from boreal wetland catchments, where water distribution reflects the interaction between relatively fixed flowpath geometry and spatially variable water table response to changing water availability (Devito et al., 2017; Elmes et al., 2021; Lambert et al., 2022).

Under headwater conditions, where higher elevation landscape position limits lateral inputs and promotes downgradient losses (i.e., Swamp 2 and the elevated portions of Bog 1; Table 1, Figures 1, A2), hydrological dynamics were controlled primarily by local storage capacity and underlying mineral permeability. In Swamp 2, relatively thin peat deposits limited the ecohydrological buffering to drying (Waddington et al., 2015), while a comparatively permeable mineral substrate acted as a “leaky” aquitard (Figure 3) and promoted drainage losses. Together with the absence of lateral gradient reversals (Table 1), these controls produced highly variable water tables and only limited near-surface saturation (Figure 2), consistent with other shallow peat and headwater wetlands

https://doi.org/10.5194/egusphere-2026-3284
Preprint. Discussion started: 19 June 2026

sensitive to climatic extremes (Åhlén et al., 2022; Rezaeianzadeh et al., 2018). Extended periods of water table drawdown (Figure 2), particularly during the June 2024 drought, likely increased oxygen exposure and decomposition potential (Strack & Waddington, 2007), thereby constraining further peat accumulation. Similar structural limitations on peat accumulation in headwater swamps have been observed in other boreal and temperate settings (Locky et al., 2005; McCarter et al., 2024), and highlight the vulnerability of shallow peat carbon stocks to increasingly frequent and intense droughts (Furukawa et al., 2025; Moore et al., 2021; Sutton et al., 2025).

In contrast, the instrumented portion of the Bog 1 dome (3A), despite occupying a similar landscape position as Swamp 2 (Figure A2), showed more stable water tables under the same external forcing. Greater peat thickness likely increased storage capacity and enhanced the internal resistance of the peat profile to water table decline (Waddington et al., 2015), allowing the water table to occupy the acrotelm 15–35% more often than in Swamp 2 (Figure 2). This likely promoted more frequent near-surface connectivity while also reducing exposure of peat to oxygenation and decomposition.

Further downslope, between 3A and 2A, the system transitioned into a hydrologically distinct zone consistent with the poor fen–bog continuum (Rydin & Jeglum, 2013). This reach exhibited both discharge and recharge behavior (Table; Figure A7) and pH values that varied from bog-like (<4.5) to fen-like (>5.0) (Figures 5, A12). These patterns suggest variable upgradient contributions from Bog 1, likely including episodic fill-and-spill inputs during snowmelt and rainfall events (Figure 2), as also suggested by the persistent similarity in near-surface SPC, pH, temperature, and DOC between 3A and 2A relative to other nests (Figures 5- 6). With continued peat accumulation and sustained connectivity, such a zone could evolve toward more distinct patterned poor fen morphology typical of the Hudson Plains (Glaser et al., 2004a, 2004b). In this higher relief setting, however, strong lateral gradients and repeated water table drawdown likely limit the expression of fen patterning.

At the outlet lagg swamp (Swamp 1), thicker peat deposits (Table 1), high and relatively stable water tables (Figure 2) and more complex geochemical signatures developed (Figures 5, A11-13), consistent with unconfined “peaty forest” lagg swamps described in eastern Canada and coastal British Columbia (Howie & van Meerveld, 2011, 2016; Langlois et al., 2015; Paradis et al., 2015). Despite slow apparent lateral inputs from upgradient units (Figure 3), particularly during acrotelm desaturation over the 2024 drought (Figure 2), hydraulic gradients remained directed from 1A toward the lake (Table 1; Figure A7). This differs from many lagg systems, where exchange with adjacent surface water can be bidirectional (Howie & van Meerveld, 2016; Langlois et al., 2015). Moreover, sustained discharge at the groundwater spring remained responsive to rainfall even when upgradient units were largely disconnected (Figures 2, 4), indicating that connectivity in this lower portion of the catchment is not governed primarily by fill-and-spill dynamics alone.

4.3 Subsurface Preferential Flowpaths as a Mechanism for Hydrological Connectivity

Rapid groundwater spring discharge and sustained outlet connectivity cannot be explained by the conventional flowpaths characterized along the transect (Figure 3). Although a localized zone of elevated K_{sat} was observed beneath 2A and 3A, consistent with poorly decomposed woody horizons or depositional heterogeneity (Balliston et

https://doi.org/10.5194/egusphere-2026-3284
Preprint. Discussion started: 19 June 2026

al., 2018; Morris et al., 2011; Rezanezhad et al., 2016b), modelled flow velocities within this zone remained insufficient to explain the rapid discharge observed at the outlet.

This discrepancy suggests the presence of preferential flowpaths not captured by modelling based solely on locally measured K_{sat} values. Evidence for this emerges from the behaviour of the groundwater spring, where discharge was more strongly correlated with deeper water table dynamics beneath Bog 1 and Swamp 2 than with local water tables at 1A (Figures A9 – A10). Groundwater spring geochemistry further supports this interpretation. In matrix-dominated flow systems, longer residence times typically promote solute exchange with the underlying mineral sediments, resulting in lower temperatures, higher SPC, and buffered pH (Fraser et al., 2001; Rezanezhad et al., 2016). In contrast, groundwater spring waters were cooler than shallow peat waters (Figures 5, A3, A13), but low in SPC and acidic in pH (Figures 5, A11, A12). This combination is more consistent with rapid subsurface transport that remains connected to upslope peat waters leading to insufficient residence time for significant mineral interaction. Modelled flowpath geometry is consistent with this interpretation (Figure 3), showing flow descending beneath Swamp 2 and Bog 1 near 3A before rising upward toward the groundwater spring near 1A.

This behaviour parallels documented macroscale preferential flowpaths, or peat pipes, reported in peatlands globally, including subarctic Yukon systems (Carey & Woo, 2000), domed bogs in the northern USA (Moore et al., 2024), and UK blanket bogs (Cunliffe et al., 2013; Holden et al., 2012; Holden & Burt, 2002; Smart et al., 2013). These conduits, often up to tens of centimeters in diameter, occur at peat-substrate interfaces or within the peat, facilitate rapid transmission of water, and can operate independently of surface saturation through pressure redistribution within the saturated zone (Carey & Woo, 2000; Holden & Burt, 2002; Smart et al., 2013).

In sloping peatlands, pipe formation has been linked to the buildup of hydraulic pressure where downslope flow is locally restricted by low-conductivity substrates, promoting transport through pressurized conduits rather than through the surrounding matrix (Carey & Woo, 2000; Holden & Burt, 2002). Evidence consistent with such a mechanism is present at nest 4A, where persistent upward hydraulic gradients between mineral and peat layers—despite its position at a topographic high—indicate overpressure at this interface (Table 1; Figure A7). Vegetation may further enhance conduit development, with root networks promoting pathway formation or connectivity between deeper preferential pathways and the surface (Cunliffe et al., 2013; Holden, 2005; Holden & Burt, 2002; Weyman, 1975). Both Swamps 1 and 2 exhibit dense woody vegetation (Figure A15a), and localized pools of cold groundwater >50 cm bgs were observed between *Sphagnum* hummocks (Figure A15b, c), consistent with preferential discharge.

Although the precise source area feeding the groundwater spring, and the broader extent of these preferential pathways remain uncertain, rapid subsurface connectivity is supported by Moose Cree First Nation Traditional Ecological Knowledge, which describes subsurface channels linking lakes and wetlands and accessed by muskrat pathways. This perspective strengthens the plausibility of a regionally connected, pressurized subsurface flow network operating beyond matrix-dominated hydrological assumptions.

https://doi.org/10.5194/egusphere-2026-3284
Preprint. Discussion started: 19 June 2026

4.4 Seasonality, water availability and preferential flow drive DOC accumulation and export

DOC concentrations in Bog 1 (Figure 6) fell within the range reported for natural bog and poor fen systems elsewhere in Canada, including sites in the adjacent Hudson Plains (Glaser et al., 2004a; Ulanowski & Branfireun, 2013), the St. Lawrence Lowlands (Blodau et al., 2007; Fraser et al., 2001) and the Precambrian Shield (Moore et al., 2003). In contrast, DOC concentrations in Swamps 1 and 2 occupied the upper end of the limited published range for swamp systems (Davidson et al., 2022) and were most consistent with values reported from coniferous organic swamps dominated by *Picea* species (McLaughlin et al., 1994; Yavitt, 1994).

Across the transect, seasonal DOC dynamics followed well-documented trajectories. Low concentrations in spring (Figure 6a, d) likely reflected dilution by low-DOC snowmelt inputs (Fraser et al., 2001; Moore, 2009; Roulet et al., 2007), followed by summer increases as declining water tables enhanced oxygen availability and microbial activity (Blodau et al., 2007; Roulet et al., 2007). These dynamics were amplified during the exceptionally dry summer of 2024, particularly within the vulnerable shallow peat of Swamp 2 (Figure 6c). This pattern is consistent with drought-driven DOC accumulation reported in other peatland systems (Khadka et al., 2016; Ritson et al., 2017; Roulet et al., 2007), which is often followed by elevated DOC export during subsequent rainfall events.

Notably, the deep DOC plume that developed beneath Bog 1 during the dry summer extended deeper than is typically reported in peatland studies, where DOC often declines sharply below the upper 10–100 cm of the peat profile (e.g., Fraser et al., 2001; Mclaughlin et al., 1994). The formation and persistence of this plume likely reflects a combination of processes, including diffusion from the large DOC pool beneath the Bog 1 dome (Figure 6d), downward transport along subsurface flowpaths, and lateral migration via preferential flow toward the catchment outlet (Figure 3). The importance of deep preferential flow in DOC export is supported by consistently elevated DOC concentrations in groundwater spring discharge, and by the rapid increase in deep porewater DOC during the spring's temporary flow cessation in September 2024 (Figure 6c). Partial dilution of this plume the following spring (Figure 6d), and its near disappearance by August 2025 (Figure 6e) both point to the multi-year hydrologic memory of the peatland and to a likely connection between groundwater spring flow and DOC flushing from upgradient units.

To place these patterns in a catchment-scale context, first-order estimates of pathway-specific water and DOC export to Tomorrow Lake were derived for each monitoring event (Table A5) for three shoreline pathway types: direct peat–lake contact, flow through mineral substrate, and discharge from the groundwater spring. For the peat–lake and mineral–lake pathways, Darcy-based fluxes were calculated over a 1 m deep and 100 m long cross-section representing the Transect A sub-catchment outlet (Figure A1b), using measured hydraulic conductivity (Figure 3; Figures A2, A8), lateral gradients (Table 1), DOC concentrations (Figure 6), and water table position (Figure). Fluxes were then normalized to sub-catchment area (0.11 km²) and averaged across the five monitoring events (Table 3).

https://doi.org/10.5194/egusphere-2026-3284
Preprint. Discussion started: 19 June 2026

Table 3. Average ± standard deviation fluxes of water and DOC at the Transect A outlet over the five monitoring events. *Calculated over a 100 m shoreline in the soil, and normalized to a sub-catchment area of0.11 km^2 **Represents the single groundwater spring.

	Q (mmyr^{-1})	Q_{DOC} (g Cm^{-1} shore·day)	Q_{DOC} (g Cm^{-2} catchment^{-1}·yr^{-1})*
Peat shoreline	510 *(1.5 - 1,454)*	34 *(0.3 - 79)*	11 (0.1 - 26)
Mineral substrate shoreline	1.8 *(0.5 - 4.3)*	0.05 *(0.03 – 0.09)*	0.02 (0.01 – 0.03)
Groundwater Spring	92 (0 – 200)	921 ** *(0 – 1,426)*	3.1 (0 - 4.7)

When groundwater spring contributions were added to either peat–lake or mineral-lake scenarios, estimated annual runoff ranged from 94 to 602 mm yr^{-1}, and DOC export from 3.1 to 14.1 g C m^{-2} yr^{-1}. These values bracket published estimates for other peatland catchments and approach the upper range reported for Arctic and subarctic peat complexes (~10 g C m^{-2} yr^{-1}) (Fraser et al., 2001; Roulet et al., 2007), while remaining lower than those reported for swamp-dominated systems (Davidson et al., 2022). This wide range underscores the difficulty of constraining catchment-scale DOC export where connectivity varies strongly through space and time.

Despite representing only a single feature, the groundwater spring exerted a disproportionate influence on both water and DOC export from the transect, accounting for a minimum of 20% of catchment DOC outflow across the study period. This supports growing evidence that preferential subsurface pathways, including peat pipes and springs, can act as efficient conduits for peatland carbon removal in a wide range of settings and hydrological conditions (Billett et al., 2012; Holden, 2005; Holden et al., 2012). In contrast, when water tables decline into underlying mineral substrates, both runoff generation and DOC export are strongly constrained (Dawson et al., 2008). Together, these observations indicate that DOC export is dominated by uneven and episodic contributions from a small number of highly connected pathways. This layered hydrology, arising from contrasts in peat structure, variability in peat–lake contact, and the transient activation of subsurface conduits, introduces substantial complexity into catchment-scale DOC export dynamics. As a result, approaches that assume diffuse, shallow flowpaths or rely on catchment-average export coefficients (e.g., Fraser et al., 2001; Moore et al., 2003) may underestimate or mischaracterize DOC fluxes in structurally complex peatland systems.

The persistence of periodic DOC export here during all but the driest conditions, driven by subsurface flushing associated with intense rainfall events, suggests that longterm future drying may enhance DOC mobilization rather than promote its retention, contrary to earlier expectations (Pastor et al., 2003). Variability in the activation and connectivity of similar preferential pathways across the broader catchment therefore remains an important source of uncertainty, with implications for regional carbon budgets, hydrological modelling, and climate adaptation strategies in peatland-dominated landscapes. Important hydrologic extremes, including the driest pre-rainfall conditions in 2024 and peak spring snowmelt, were not sampled directly. Additional measurements during these periods are needed to better constrain DOC mobilization under extreme wet and dry conditions.

https://doi.org/10.5194/egusphere-2026-3284
Preprint. Discussion started: 19 June 2026

5.0 Conclusions

In this transitional Precambrian Shield peatland complex, water and dissolved organic carbon (DOC) movement were governed by how landscape structure organized flowpaths and how hydrologic conditions selectively activated them. From the highest points within the transect to the outflow at Tomorrow Lake, lateral hydraulic gradients remained aligned with surface topography; flowpath geometry was consistent over a wide range of hydrological conditions, indicating that flow direction is persistently constrained by landscape position, peat development, and underlying mineral stratigraphy. At the same time, activation of these flowpaths varied among wetland units as water tables rose and fell, demonstrating that peatland connectivity in this system was controlled by the interaction between stable structural organization and dynamic storage conditions, particularly peat due to its large capacity for water regulation.

Hydrological and DOC dynamics across most of the transect followed expected seasonal patterns in general, with the lowest DOC concentrations but highest near surface connectivity during spring freshet and higher DOC concentrations but reduced near surface connectivity during warm, dry periods. However, DOC accumulation during disconnected periods was not confined to the near surface. A persistent deep DOC reservoir developed beneath the bog and was later flushed toward the outlet to the lake, showing that carbon export can remain substantial even under conditions typically assumed to favour storage. At the outlet, a groundwater spring contrasted sharply with upgradient patterns, remaining highly responsive to rainfall events throughout the spring and summer. Multiple lines of evidence show that this discharge was sustained by deeper, pressurized preferential flowpaths linking upgradient wetlands to the lake margin. These pathways remained active even during dry periods when upgradient near-surface units were largely disconnected, and thus these pathways contributed disproportionately to water and DOC export to the lake.

Together, these results show that water and DOC export from intact peatland complexes in the headwaters of the Hudson Plains are governed not only by the traditionally recognized near-surface fill-and-spill connectivity, but also by structurally organized deeper preferential pathways. They also highlight the limitations of remote sensing and generalized landscape datasets for identifying the small-scale subsurface features that exert important controls on hydrology and carbon transport in transitional peatland terrain. As hydroclimatic variability and disturbance intensify across the boreal, deep DOC storage and episodic export through preferential pathways are likely to become increasingly important controls on downstream water quality and carbon flux. This is particularly important in transitional Shield–Hudson Plains terrain, where overlooked peatland complexes may become critical controls on the hydrological and carbon consequences of future development, including in regions such as the Ring of Fire.

https://doi.org/10.5194/egusphere-2026-3284
Preprint. Discussion started: 19 June 2026

Appendix A

Table A1. Monthly average temperature, total precipitation and average snow depth for the years of 2024 and 2025 in comparison to 30 year climate normals (1991-2020). Highlighted months indicate conditions more than one standard deviation from the norm (red indicates hotter/ drier and blue colder/ wetter) while bolded values indicate values 2 standard deviations from the norm or more. Data source: Moosonee (Environment and Climate Change Canada, 2026)

		Jan	Feb	Mar	Apr	May	Jun	Jul	Aug	Sep	Oct	Nov	Dec
Avg Temp (°C)	2024	-15	-13	-6	1	10	**16**	17	17	**15**	5	-1	-12
	2025	-19	-19	-12	-2	6	14	17	16	12	-	-	-
	Norm	-17	-16	-9	-1	8	14	17	16	12	4	-4	-12
Tot Precip (mm)	2024	27	23	26	49	56	55	95	32	53	84	57	24
	2025	26	26	37	83	36	**172**	83	57	36	-	-	-
	Norm	42	35	39	48	67	74	92	81	94	81	60	49
Avg Snow Depth (cm)	2024	35	37	33	6	0	0	0	0	0	0	**5**	25
	2025	36	46	**77**	41	0	0	0	0	0	-	-	-
	Norm	59	49	41	29	4	0	0	0	0	15	52	62

Table A2. Lateral hydraulic conductivity values measured using slug tests in June and August 2025 at all piezometer installations. A minimum of 20 cm of drawdown and 90% recovery was required for test completion. Tests were analyzed using the (Hvorslev, 1951) method; r^2 values indicate how well the recovery data fit the straight-line relationship used to estimate K_{sat}

LOCATION	MATERIAL	SCREENED DEPTH	DATE OF TEST	K_{SAT} (MS^{-1})	R^2
1A	peat	75	2025-05-28	4.7E-07	0.99
1A	peat	75	2025-08-28	6.6E-07	0.99
1A	mineral	100	2025-05-28	1.4E-08	0.90
1A	mineral	100	2025-08-28	2.9E-08	1.0
1A	mineral	117	2025-05-28	3.7E-09	0.97
1A	mineral	117	2025-09-16	3.1E-09	0.94
2A	peat	75	2025-05-28	7.1E-07	1.0
2A	peat	75	2025-09-16	1.1E-06	0.98
2A	peat	100	2025-05-28	1.0E-05	0.98
2A	peat	100	2025-08-28	1.8E-06	0.90
2A	peat	100	2025-09-16	2.5E-06	0.89
2A	mineral	150	2025-05-28	6.0E-09	0.86
2A	mineral	150	2025-08-28	1.6E-08	0.97
2A	peat	75	2025-05-28	8.4E-07	0.99
3A	peat	75	2025-08-25	4.1E-06	0.80
3A	peat	100	2025-05-28	1.1E-07	0.98
3A	peat	100	2025-08-25	1.6E-07	0.97
3A	peat	150	2025-05-28	1.3E-06	1.0
3A	peat	150	2025-08-25	2.4E-06	0.92
3A	peat	200	2025-05-28	1.5E-06	0.89

https://doi.org/10.5194/egusphere-2026-3284
Preprint. Discussion started: 19 June 2026

3A	peat	200	2025-08-25	6.0E-06	0.97
4A	mineral	75	2025-05-28	8.6E-07	0.98
4A	mineral	75	2025-09-16	1.0E-06	0.94
5A	peat /mineral	75	2025-05-28	2.1E-06	0.92
5A	Peat/mineral	75	2025-08-28	1.4E-06	0.87

645 **Table A3. Vertical hydraulic gradients calculated for each field campaign between the shallowest and deepest hydraulic head measurements at the time of sampling (generally between the water table and the deepest installation). Positive values indicate upwards flow.**

	SWAMP 1		**BOG 1**	**SWAMP 2**	
	1A	2A	3A	4A	5A
JUN-24	-2.4	3.9	-4.3	7.3	-21.7
AUG-24	0.0	1.6	-2.4	17.1	11.8
SEP-24	-2.3	1.7	0.6	29.6	28.6
JUN-25	1.9	-0.8	-0.6	8.0	-3.7
AUG-25	-8.8	-0.8	-3.0	-5.9	-20.0
SEP-25	1.1	5.0	-0.6	29.2	-22.2
AVERAGE	-1.7	1.8	-1.7	14.2	-4.6
STDEV	3.9	2.4	1.8	13.9	21.0

https://doi.org/10.5194/egusphere-2026-3284
Preprint. Discussion started: 19 June 2026

Table A4. Integrated pH, specific conductance (SPC) and water temperature (average ± standard deviation) over the entire peat profile at 1A.

Date	Field Parameters Groundwater Outflow (Soil) pH (-)	SPC (μScm^{-1})	Temperature (°C)
Jun-24	6.3 ± 0.4	152 ±129	9 ±1
Aug-24	6.1 ± 0.6	142 ±120	12 ±2
Sep-24	6.2 ± 0.6	151 ±106	16 ±1
Jun-25	5.9 ± 0.7	127 ±88	9 ±1
Aug-25	6.0 ± 0.7	119 ±95	13 ±2
Average	6.2 ± 0.6	113 ±107	12 ±1

Table A5. Water and DOC flux per meter of interface between adjacent wetland types, or per meter shoreline at the Swamp 1 outlet. *Flow rates for the groundwater spring are in L/d. Cross sectional areas were calculated as the average peat depth in the wetland unit, and length of intersection between adjacent units (300m, 100m and 100 m from Swamp 2/ Bog 1, Bog 1/ Swamp 1 and the outlet, respectively assessed using aerial imagery and known shifts in wetland type).

		Q ($Lm^{-1}d^{-1}$)	Q_{DOC} (g m·$shore^{-1}$ day^{-1})	Q_{DOC} (g m^2 ·$catchment^{-1}yr^{-1}$)
Jun-24	Outlet (peat)	1,731	33.5	11.1
	Outlet (sand/gravel/silt)	6.0	0.03	0.01
	Groundwater spring	43,200	1,426	4.7
Aug-24	Outlet (peat)	449.64	14.6	4.8
	Outlet (sand/gravel/silt)	2.68	0.04	0.01
	Groundwater spring	12,960	505	1.7
Sep-24	Outlet (peat)	4.6	0.28	0.09
	Outlet (sand/gravel/silt)	1.5	0.09	0.03
	Groundwater spring	0	0	0
Jun-25	Outlet (peat)	4,380	79.3	26.3
	Outlet (sand/gravel/silt)	12.9	0.03	0.01
	Groundwater spring	60,480	1,391	4.6
Aug-25	Outlet (peat)	1,117.	43.5	14
	Outlet (sand/gravel/silt)	4.4	0.05	0.02
	Groundwater spring	22,464	1,280	4.3

https://doi.org/10.5194/egusphere-2026-3284
Preprint. Discussion started: 19 June 2026

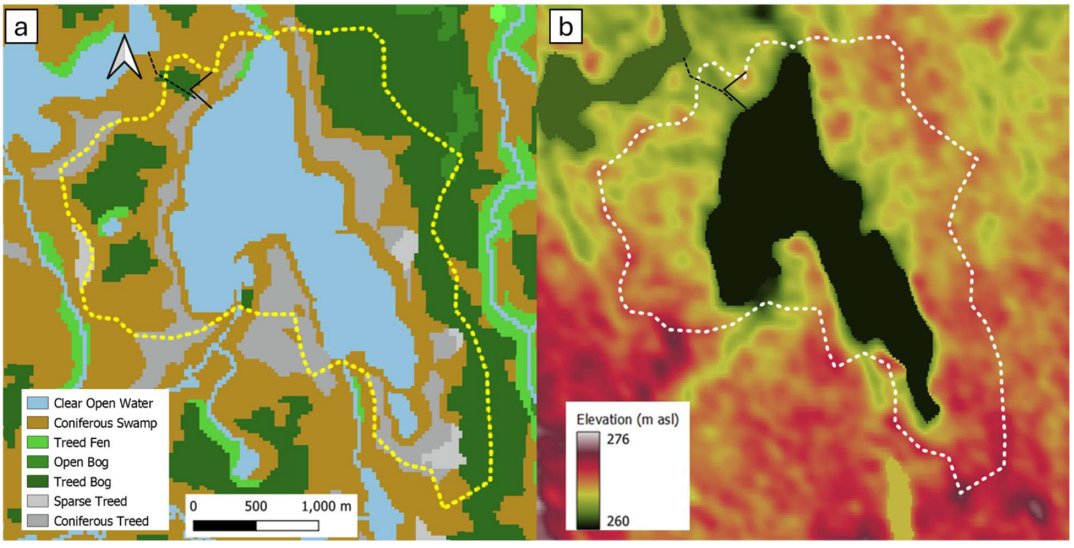

Figure A1. The Tomorrow Lake a) Land cover classifications in accordance with Far North Land Cover data (OMNRF, 2014) and b) ground elevation in accordance with the Canadian Digital Surface Model (NRCan, 2000). Transects are delineated with black lines and the catchment with dashed yellow/ white.

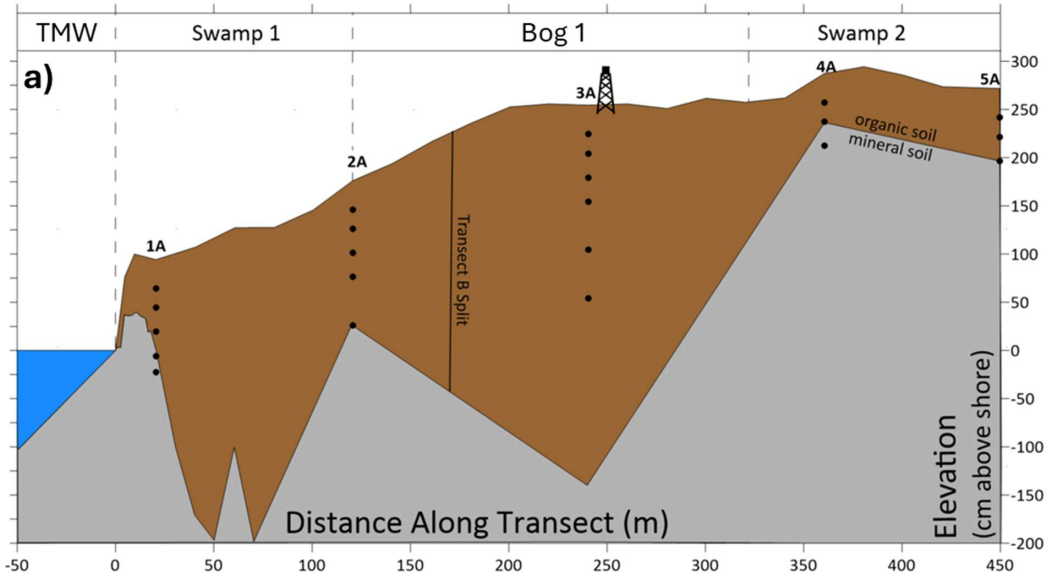

https://doi.org/10.5194/egusphere-2026-3284
Preprint. Discussion started: 19 June 2026

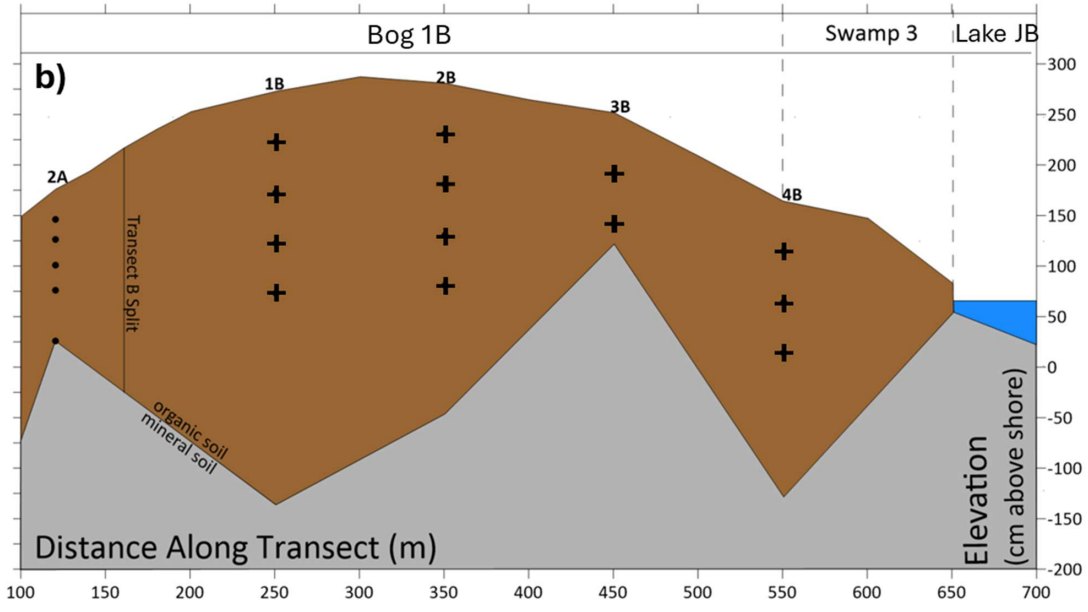

Figure A2. a) Transect originating at a topographical high at Swamp 2, travelling through Bog 1 and flowing through Swamp 1 and into Tomorrow Lake and b) 2025- Extending from Nest 2 at Transect A, past a secondary topographical high within the main bog/ fen (Bog 1B) and through Swamp 3 terminating at a secondary lake (Lake JB) outside of the Tomorrow Lake catchment area. Hydrological/ biogeochemical installations occurred at numbered nests at depths indicated by black circles (permanent installations) and crosses (temporary water samplers). The meteorological station (tower symbol) was installed at nest 3A.

https://doi.org/10.5194/egusphere-2026-3284
Preprint. Discussion started: 19 June 2026

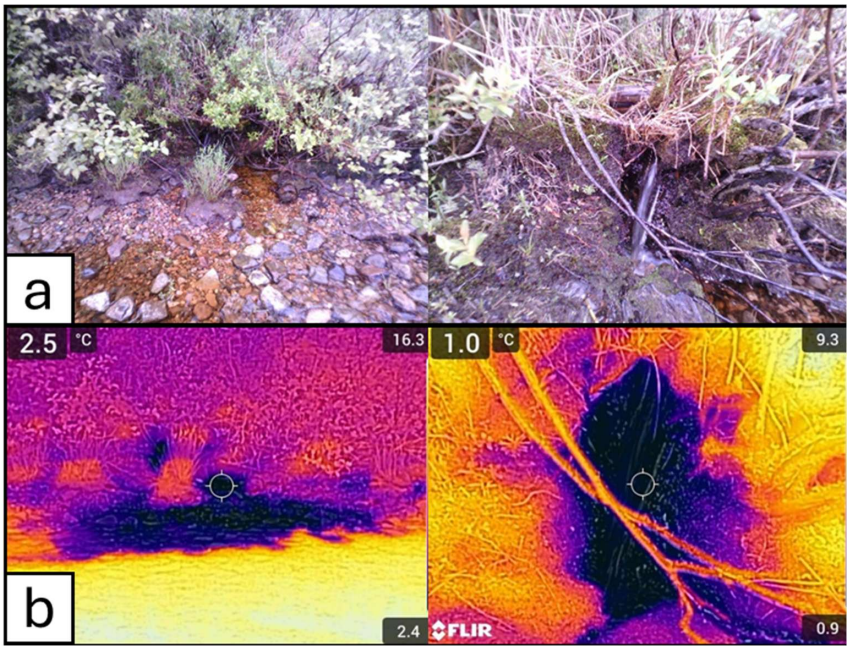

Figure A3. a) Photos of stream-like groundwater spring at the transect shoreline discovered during transect installation in June 2024. A FLIR thermal imagining camera was then used to capture outflow water temperatures at this location b) which was determined to be ~ 14°C colder than the adjacent surface water of Tomorrow Lake

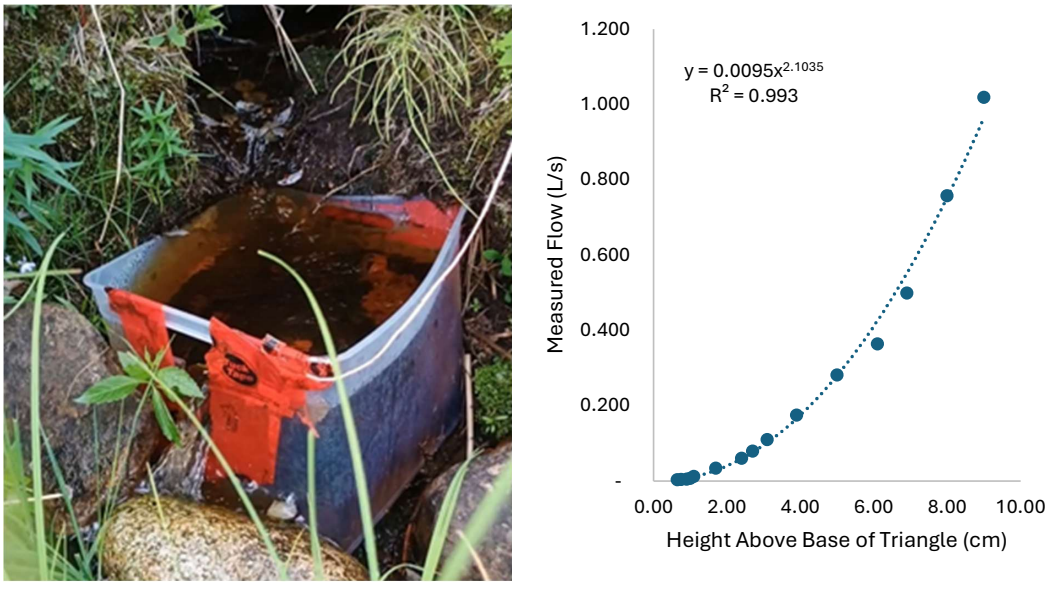

Figure A4. a) V-notch bucket weir installed at the groundwater spring in spring 2025 ~5 m from the intersection point between the transect and Tomorrow Lake, fitted with a HOBO U20L water level logger,

https://doi.org/10.5194/egusphere-2026-3284
Preprint. Discussion started: 19 June 2026

and b) the associated stage-discharge curve used to generate continuous flow data. The maximum flow capacity of the weir before overflow is 1 Ls^{-1}

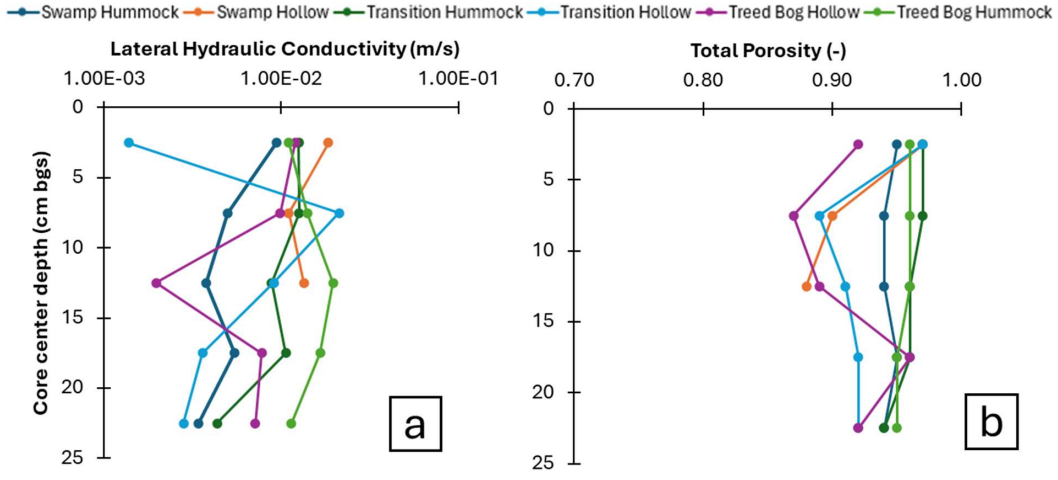

Figure A5. a) Lateral hydraulic conductivity (ms^{-1}) and b) total porosity (-) measured in five centimeter increments in six peat cores representing the top 25 cm of the peat profile. Cores were taken from representative cover types across Transect A and used to parameterize the Topodrive flow model

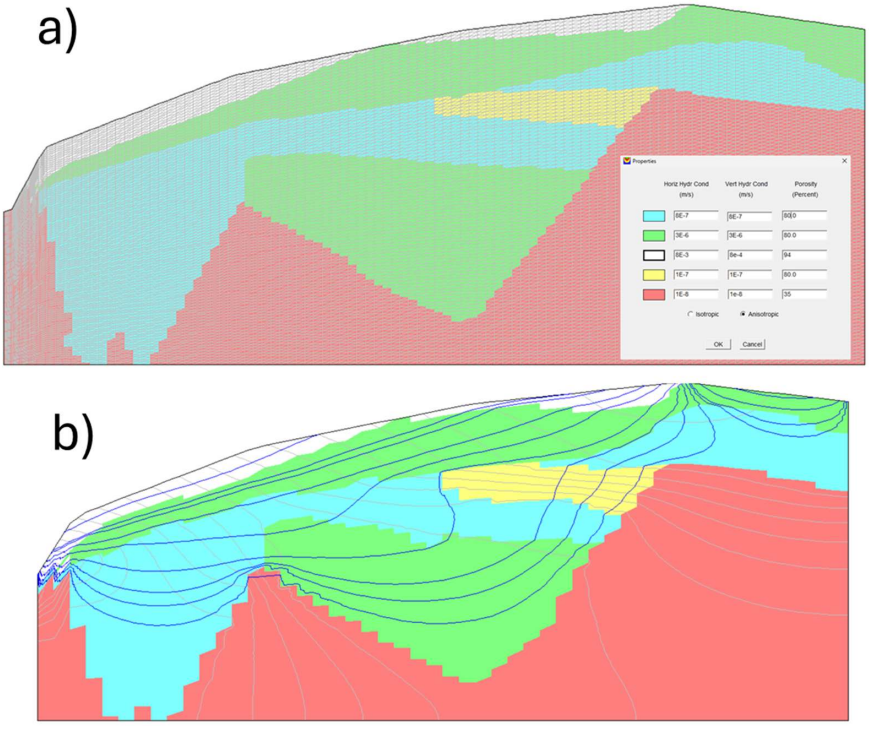

https://doi.org/10.5194/egusphere-2026-3284
Preprint. Discussion started: 19 June 2026

Figure A6. a) Topodrive parameterization and b) resulting flownet and flowpath tracking ouput generated using shallowest measured water table depths, lab measured porosity and lab and field measured lateral hydraulic conductivity values.

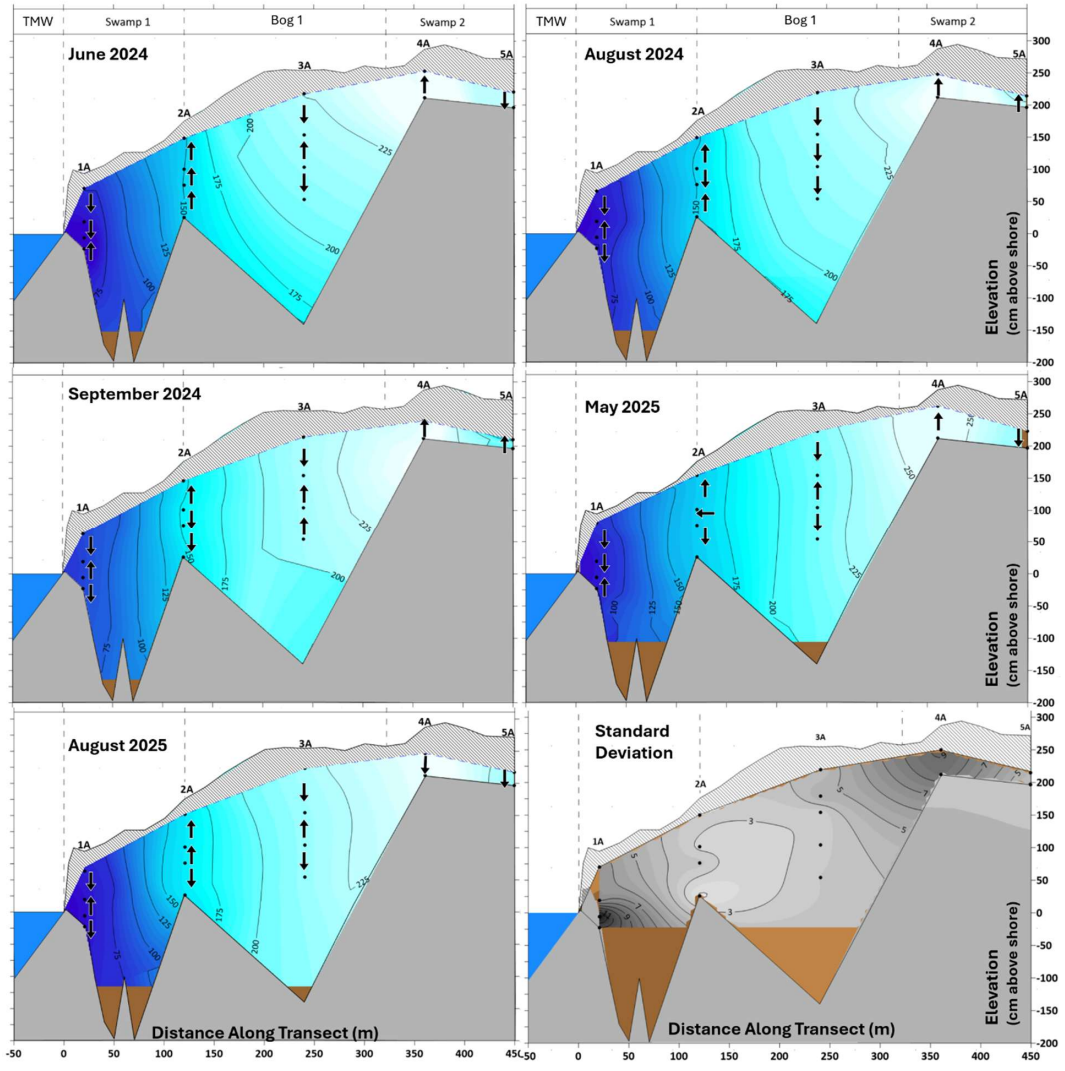

Figure A7. Surfer hydraulic head contour maps generated for each monitoring event using manual values collected over the 2024-2025 monitoring period in piezometers installed at each nest at 75, 100, 150 and 200 cm (or until mineral reached). Black arrows indicate the direction of the vertical hydraulic gradient between the closest two monitoring points.

https://doi.org/10.5194/egusphere-2026-3284
Preprint. Discussion started: 19 June 2026

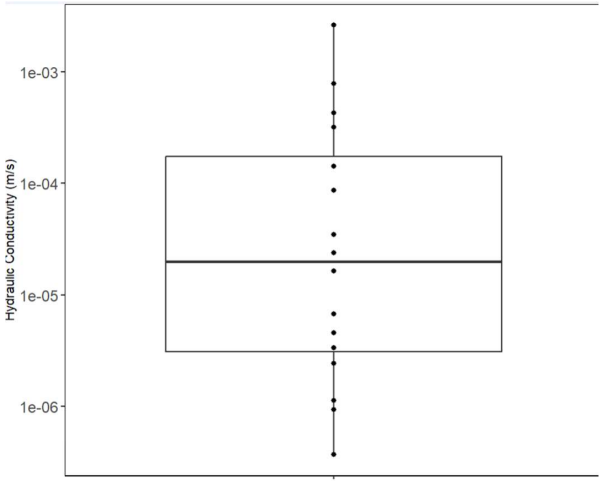

Figure A8. Hydraulic conductivity values measured using falling head test in near shore shallow mineral soils taken from the peat/ mineral interface in the last 10 m of transect where it intersects Tomorrow Lake

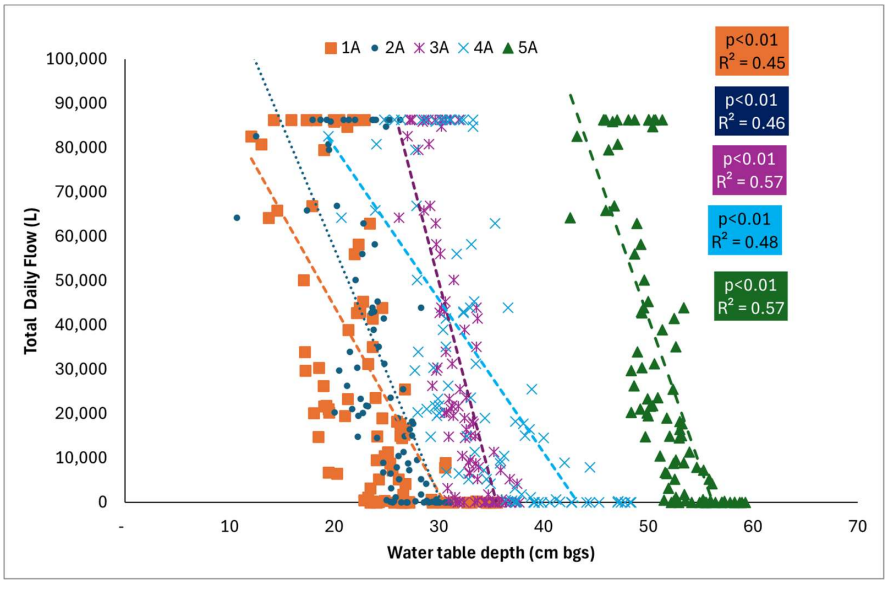

Figure A9. Linear regressions between average daily flows at the groundwater spring and the five upgradient monitoring wells along Transect A

https://doi.org/10.5194/egusphere-2026-3284
Preprint. Discussion started: 19 June 2026

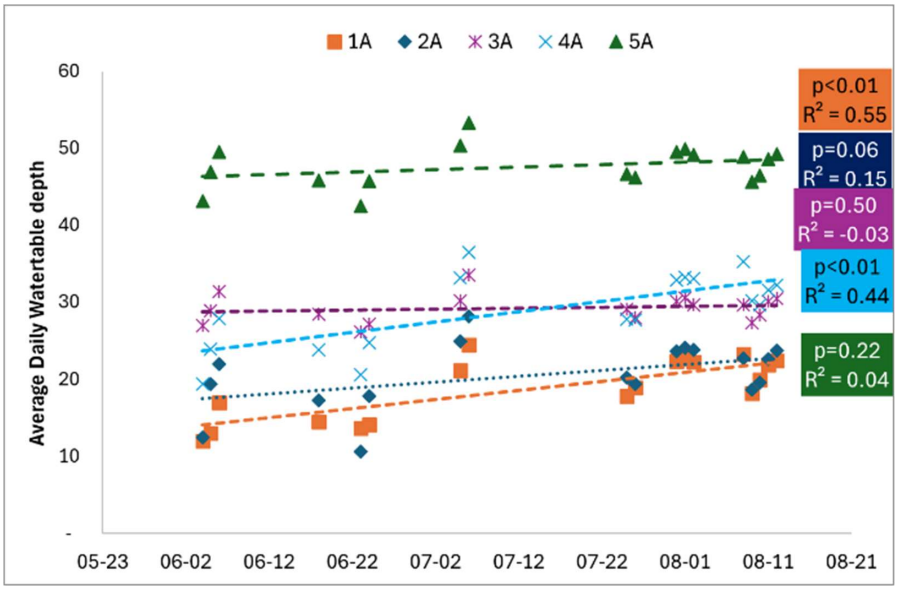

Figure A10. a) regression between water table depth and time during high flow periods within the outlet weir Regressions show a general deepening of water tables associated with high flow conditions as the summer progressed, though this was only statistically significant (p<0.01) at 1A and 4A.

https://doi.org/10.5194/egusphere-2026-3284
Preprint. Discussion started: 19 June 2026

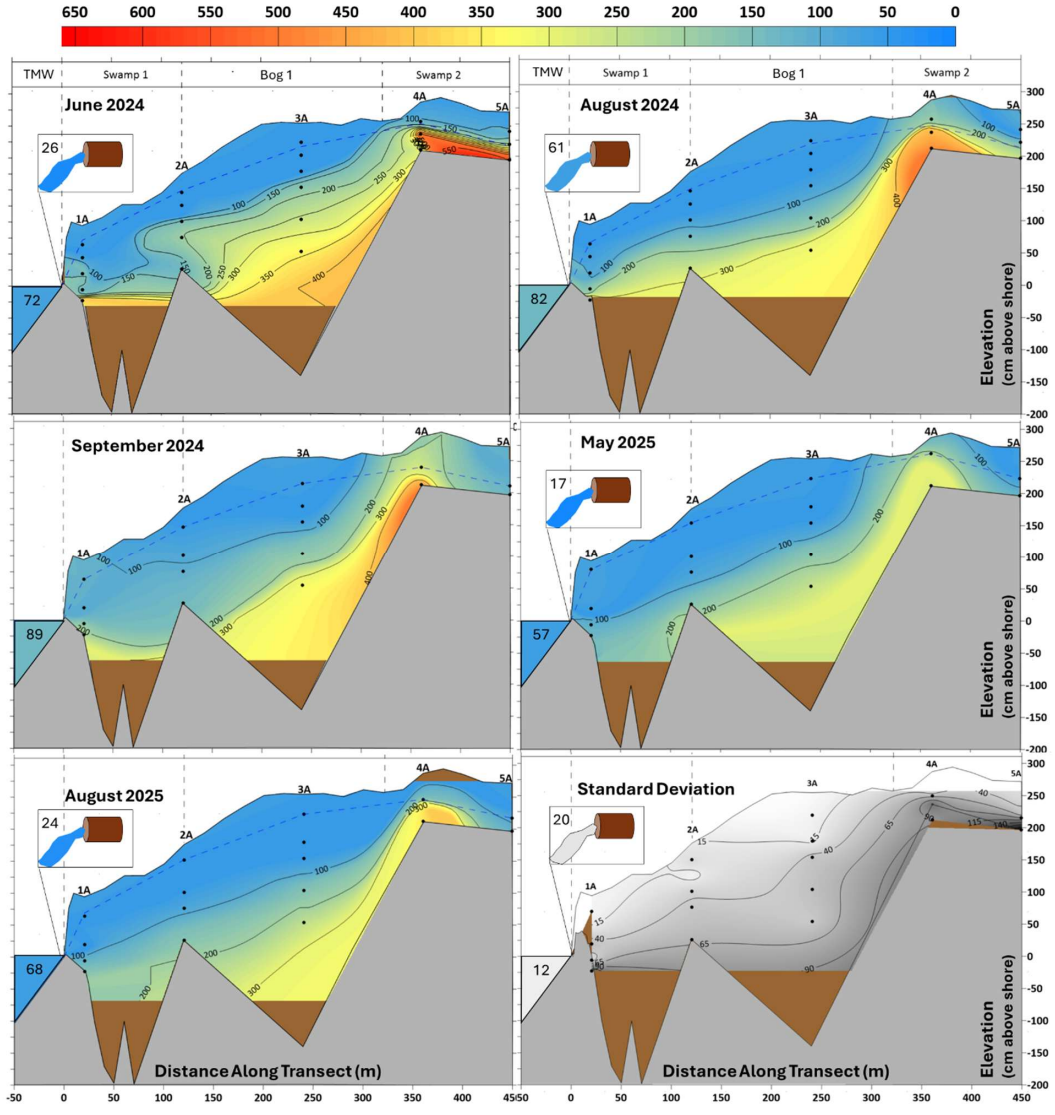

Figure A11. Porewater and surface water specific conductivity (µSc^{-1}m) contours generated for each monitoring event across Transect A and the groundwater spring using Surfer and manual interpolation, as well as the standard deviation across all monitoring events

https://doi.org/10.5194/egusphere-2026-3284
Preprint. Discussion started: 19 June 2026

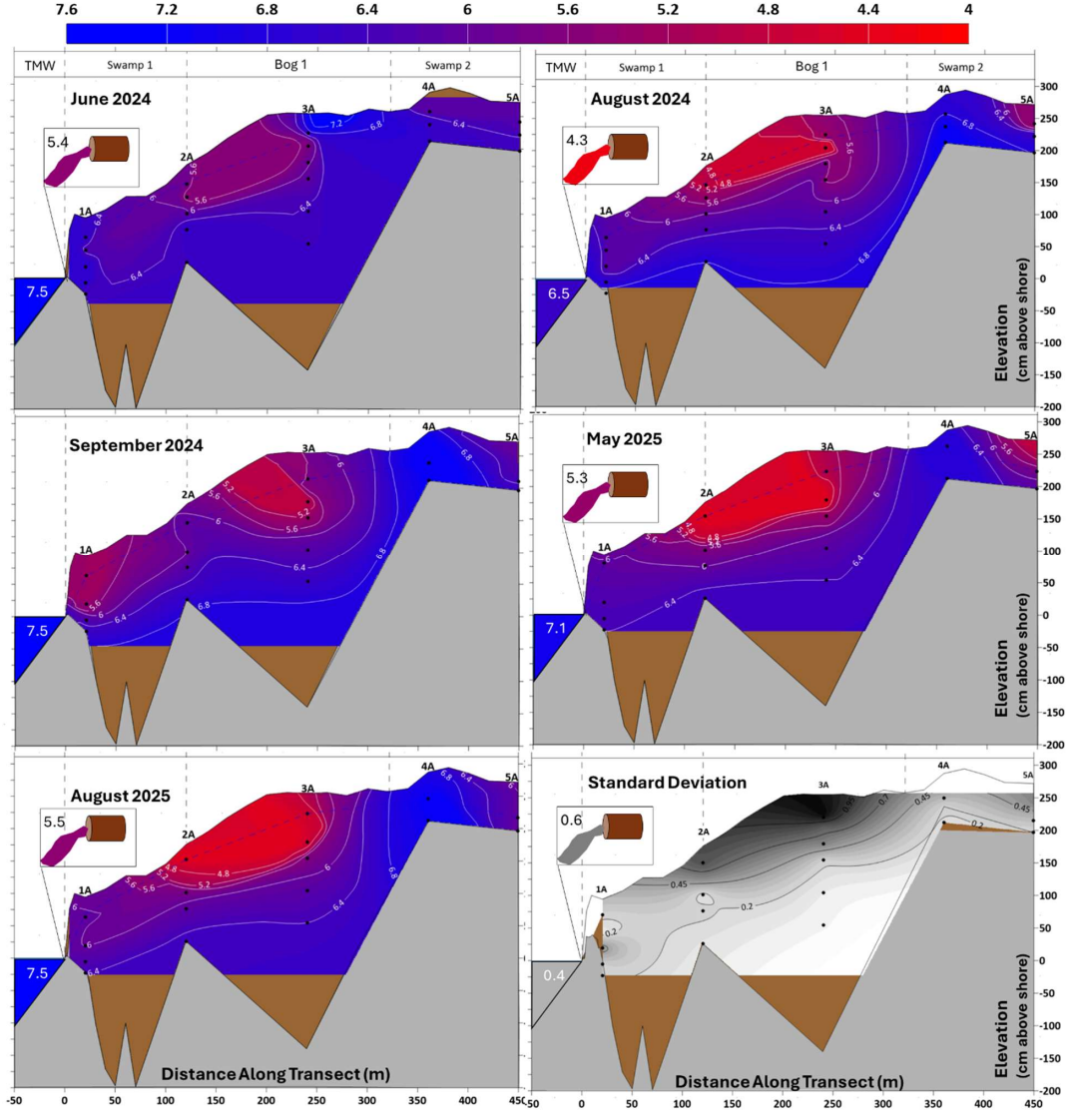

Figure A12. Porewater and surface water pH (-) contours generated for each monitoring event across Transect A and the groundwater spring using Surfer and manual interpolation, as well as the standard deviation across all monitoring events

https://doi.org/10.5194/egusphere-2026-3284
Preprint. Discussion started: 19 June 2026

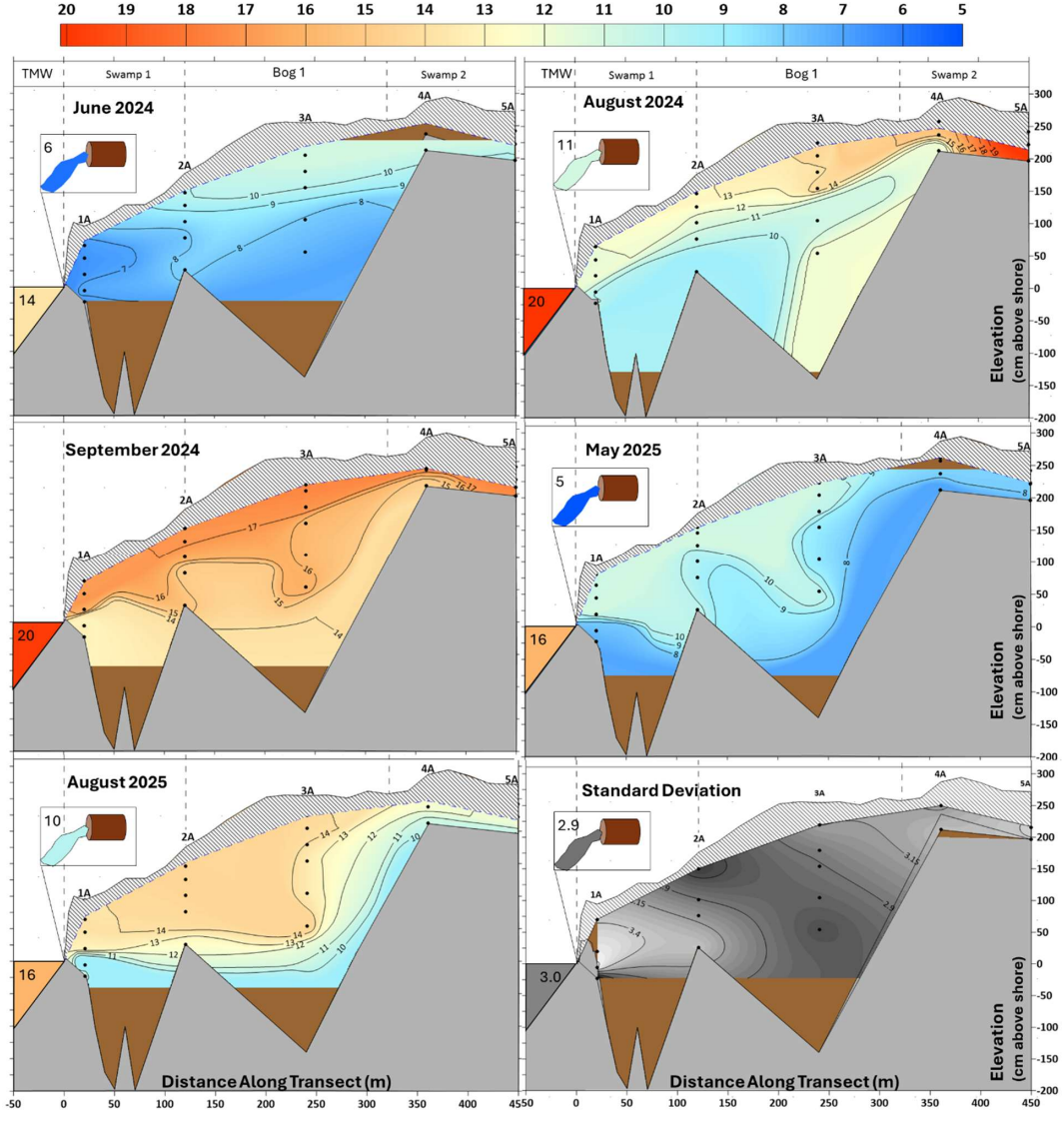

Figure A13. Porewater and surface water temperature (°C) contours generated for each monitoring event across Transect A and the groundwater spring using Surfer and manual interpolation, as well as the standard deviation across all monitoring events

https://doi.org/10.5194/egusphere-2026-3284
Preprint. Discussion started: 19 June 2026

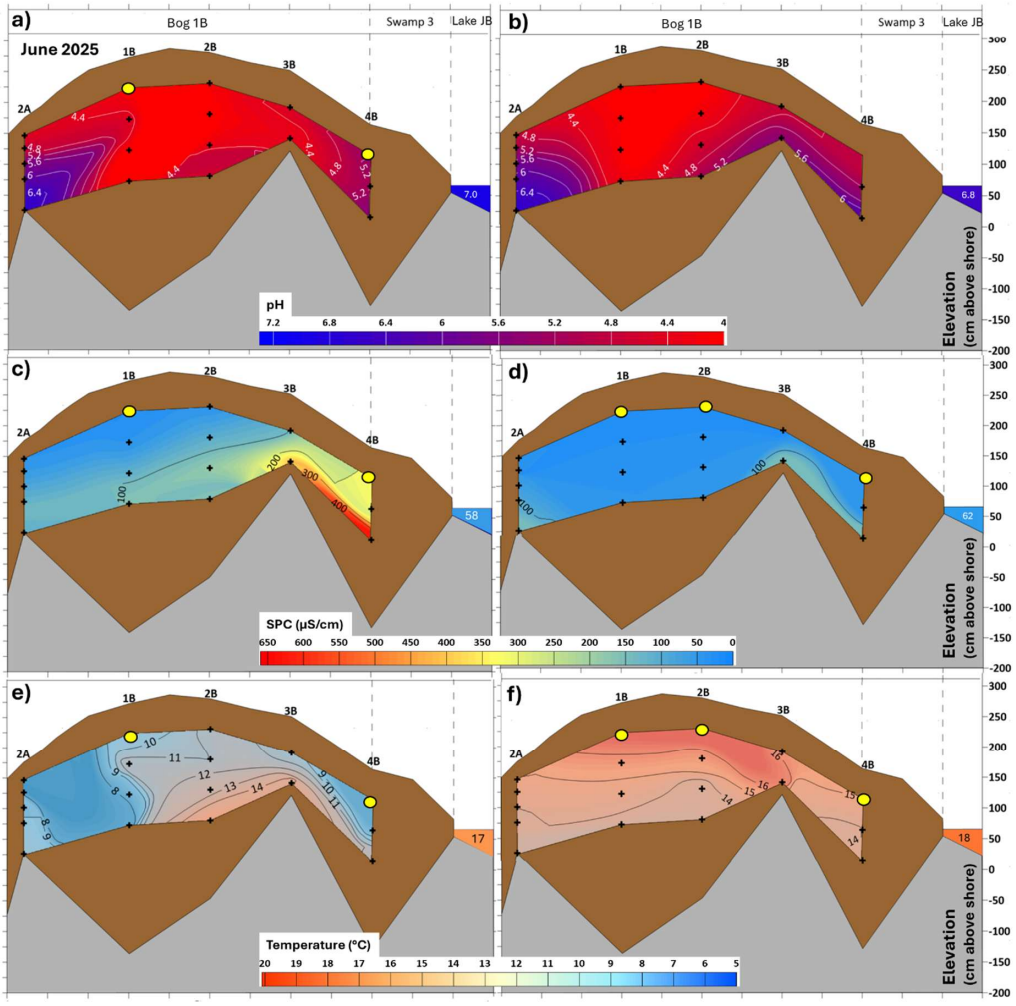

Figure A14. Transect B contours depicting a,b) pH (-) c,d) specific conductance (SPC- µScm^{-1}), and e,f) temperature (- °C) for the June 2025 (left) and August 2025 (right) monitoring events *Note depths indicated with a yellow circle were above the water table, porewater was squeezed from peat at this depth to obtain a sample.

https://doi.org/10.5194/egusphere-2026-3284
Preprint. Discussion started: 19 June 2026

Figure A15. a) Photograph taken from a small clearing adjacent to 1A showing Swamp 1 dense tree cover with an understory of shrubs and Sphagnum mosses, b) opening in Sphagnum hummock revealing pooled water ~ 30 cm below the ground surface with c) associated cold water signature indicative of deep groundwater connectivity observed in Swamp 1 adjacent to the 1A nest and captured via FLIR thermal camera.

https://doi.org/10.5194/egusphere-2026-3284
Preprint. Discussion started: 19 June 2026

Data Availability

The data supporting this study have been deposited in Borealis, the Canadian Dataverse Repository, at https://doi.org/10.5683/SP4/AR80IE. At this time, access to the dataset is restricted because the data were collected in partnership with Moose Cree First Nation and include information that may be sensitive in the context of Indigenous data governance, community priorities, and place-based environmental knowledge. Access may be requested through the Borealis repository and will be considered on a case-by-case basis in accordance with the terms of access and in consultation with the relevant data partners where appropriate.

Author contributions

N.B. conceptualized the study, conducted field investigations, performed formal analysis, and wrote the original draft. M.V. and J.H. contributed to methodology development, field investigations, and writing – review and editing. S.F. contributed to conceptual development, data interpretation, and writing – review and editing. M.S. provided supervision and contributed to writing – review and editing.

Conflicts of Interest

The authors declare that they have no conflict of interest.

Acknowledgments

This study would not have been possible without the guidance, knowledge, and generosity of Moose Cree First Nation collaborators John Turner, Ron Spencer, Thomas Echum, and especially Clarence Trapper. Clarence's deep knowledge of the land guided the selection of the study site and helped shape the research questions explored here. The partnership and support of Moose Cree First Nation were foundational to this work. The authors also gratefully acknowledge Mushkegowuk Council for their collaboration and support. The authors further thank Ruth Hall, Grace Calloway, Syd Higgins, Miranda Hunter, Maryam Bayatvarkeshi, and Rayden Laliberte for field and logistical assistance.

Financial support

Funding was provided by Parks Canada and Environment and Climate Change Canada under the Hudson Bay Biodiversity and Carbon Sequestration Initiative.

References

Åhlén, I., Thorslund, J., Hambäck, P., Destouni, G., & Jarsjö, J. (2022). Wetland position in the landscape: Impact on water storage and flood buffering. *Ecohydrology*, *15*(7), e2458. https://doi.org/10.1002/eco.2458

Aho, K. S., & Raymond, P. A. (2019). Differential Response of Greenhouse Gas Evasion to Storms in Forested and Wetland Streams. *JGR Biogeosciences*, *124*(3), 649–662. https://doi.org/10.1029/2018JG004750

https://doi.org/10.5194/egusphere-2026-3284
Preprint. Discussion started: 19 June 2026

Balliston, McCarter, C., & Price, J. (2018). Microtopographical and hydrophysical controls on subsurface flow and solute transport: A continuous solute release experiment in a subarctic bog. *Hydrological Processes*, *32*(19), 2963–2975. https://doi.org/10.1002/hyp.13236

Balliston, & Price, J. S. (2022). Beyond fill and spill: Hydrological connectivity in a sub-arctic bog-fen-tributary complex in the Hudson Bay Lowlands, Canada. *Hydrological Processes*, *36*(4), e14575. https://doi.org/10.1002/hyp.14575

Basiliko, N., Blodau, C., Roehm, C., Bengtson, P., & Moore, T. R. (2007). Regulation of Decomposition and Methane Dynamics across Natural, Commercially Mined, and Restored Northern Peatlands. *Ecosystems*, *10*(7), 1148–1165. https://doi.org/10.1007/s10021-007-9083-2

Beckwith, C. W., Baird, A. J., & Heathwaite, A. L. (2003). Anisotropy and depth-related heterogeneity of hydraulic conductivity in a bog peat. I: Laboratory measurements. *Hydrological Processes*, *17*(1), 89–101. https://doi.org/10.1002/hyp.1116

Billett, M. F., Dinsmore, K. J., Smart, R. P., Garnett, M. H., Holden, J., Chapman, P., Baird, A. J., Grayson, R., & Stott, A. W. (2012). Variable source and age of different forms of carbon released from natural peatland pipes. *Journal of Geophysical Research: Biogeosciences*, *117*(G2), 2011JG001807. https://doi.org/10.1029/2011JG001807

Blodau, C., Roulet, N. T., Heitmann, T., Stewart, H., Beer, J., Lafleur, P., & Moore, T. R. (2007). Belowground carbon turnover in a temperate ombrotrophic bog. *Global Biogeochemical Cycles*, *21*(1). https://doi.org/10.1029/2005GB002659

Branfireun, B. A., & Roulet, N. T. (1998). The baseflow and storm flow hydrology of a precambrian shield headwater peatland. *Hydrological Processes*, *12*(1), 57–72. https://doi.org/10.1002/(SICI)1099-1085(199801)12:1%253C57::AID-HYP560%253E3.0.CO;2-U

Carey, S. K., & Woo, M.-K. (2000). The role of soil pipes as a slope runoff mechanism, Subarctic Yukon, Canada. *Journal of Hydrology*, *233*(1), 206–222. https://doi.org/10.1016/S0022-1694(00)00234-1

Clark, J. M., Lane, S., Chapman, P., & Adamson, J. (2007). Export of dissolved organic carbon from an upland peatland during storm events: Implications for flux estimates. *Journal of Hydrology*, *347*(3–4), 438–447.

https://doi.org/10.5194/egusphere-2026-3284
Preprint. Discussion started: 19 June 2026

Connon, R. F., Quinton, W. L., Craig, J. R., Hanisch, J., & Sonnentag, O. (2015). The hydrology of interconnected bog complexes in discontinuous permafrost terrains. *Hydrological Processes*, *29*(18), 3831–3847. https://doi.org/10.1002/hyp.10604

Creed, I. F., Bergström, A., Trick, C. G., Grimm, N. B., Hessen, D. O., Karlsson, J., Kidd, K. A., Kritzberg, E., McKnight, D. M., Freeman, E. C., Senar, O. E., Andersson, A., Ask, J., Berggren, M., Cherif, M., Giesler, R., Hotchkiss, E. R., Kortelainen, P., Palta, M. M., … Weyhenmeyer, G. A. (2018). Global change-driven effects on dissolved organic matter composition: Implications for food webs of northern lakes. *Global Change Biology*, *24*(8), 3692–3714. https://doi.org/10.1111/gcb.14129

Cunliffe, A. M., Baird, A. J., & Holden, J. (2013). Hydrological hotspots in blanket peatlands: Spatial variation in peat permeability around a natural soil pipe: S. *Water Resources Research*, *49*(9), 5342–5354. https://doi.org/10.1002/wrcr.20435

Davidson, S. J., Dazé, E., Byun, E., Hiler, D., Kangur, M., Talbot, J., Finkelstein, S. A., & Strack, M. (2022). The unrecognized importance of carbon stocks and fluxes from swamps in Canada and the USA. *Environmental Research Letters*, *17*(5), 053003. https://doi.org/10.1088/1748-9326/ac63d5

Davies, M. A., Mclaughlin, J. W., Packalen, M. S., & Finkelstein, S. A. (2022). Holocene carbon storage and testate amoeba community structure in treed peatlands of the western Hudson Bay Lowlands margin, Canada. *Journal of Quaternary Science*, *38*(1), 92–106. https://doi.org/10.1002/jqs.3465

Dawson, J. J. C., Soulsby, C., Tetzlaff, D., Hrachowitz, M., Dunn, S. M., & Malcolm, I. A. (2008). Influence of hydrology and seasonality on DOC exports from three contrasting upland catchments. *Biogeochemistry*, *90*(1), 93–113. https://doi.org/10.1007/s10533-008-9234-3

DeLancey, E. R., Kariyeva, J., Bried, J. T., & Hird, J. N. (2019). Large-scale probabilistic identification of boreal peatlands using Google Earth Engine, open-access satellite data, and machine learning. *PLOS ONE*, *14*(6), e0218165. https://doi.org/10.1371/journal.pone.0218165

Devito, Creed, I., Gan, T., Mendoza, C., Petrone, R., Silins, U., & Smerdon, B. (2005). A framework for broad-scale classification of hydrologic response units on the Boreal Plain: Is topography the last thing to consider? *Hydrological Processes*, *19*(8), 1705–1714. https://doi.org/10.1002/hyp.5881

Devito, Hokanson, K. J., Moore, P. A., Kettridge, N., Anderson, A. E., Chasmer, L., Hopkinson, C., Lukenbach, M. C., Mendoza, C. A., Morissette, J., Peters, D. L., Petrone, R. M., Silins, U., Smerdon, B., & Waddington, J.

https://doi.org/10.5194/egusphere-2026-3284
Preprint. Discussion started: 19 June 2026

M. (2017). Landscape controls on long-term runoff in subhumid heterogeneous Boreal Plains catchments. *Hydrological Processes*, *31*(15), 2737–2751. https://doi.org/10.1002/hyp.11213

Devito, K. J., Waddington, J. M., & Branfireun, B. A. (1997). Flow Reversals in Peatlands Influenced by Local Groundwater Systems. *Hydrological Processes*, *11*(1), 103–110. https://doi.org/10.1002/(SICI)1099-1085(199701)11:1%3C103::AID-HYP417%3E3.0.CO;2-E

Dinsmore, K. J., Billett, M. F., Skiba, U. M., Rees, R. M., Drewer, J., & Helfter, C. (2010). Role of the aquatic pathway in the carbon and greenhouse gas budgets of a peatland catchment. *Global Change Biology*, *16*(10), 2750–2762. https://doi.org/10.1111/j.1365-2486.2009.02119.x

Dredge, L., & Dyke, L. (2020). *Landscapes and Landforms of the Hudson Bay Lowlands* (pp. 211–227). https://doi.org/10.1007/978-3-030-35137-3_8

Earle, S. (2015). *Physical Geology*. BCcampus. https://opentextbc.ca/

Ekstrom, B., Breau, J., Thompson, E., Woolnough, N., & Quist, L. (2007). *Forest Management Plan for the Hearst Forest for the 10-year period from April 1, 2007 to March 31, 2017* (p. 516) [2007-2017-SFL 550053]. Hearst Forest Management Inc.,. https://www.hearstforest.com/english/PDF/HearstForest2007FMP.pdf

Elmes, M. C., Davidson, S. J., & Price, J. S. (2021). Ecohydrological interactions in a boreal fen–swamp complex, Alberta, Canada. *Ecohydrology*, *14*(7), e2335. https://doi.org/10.1002/eco.2335

Environment and Climate Change Canada. (2026). *Historical climate data: Daily data—Moosonee station* [Dataset]. https://climate-change.canada.ca/climate-data/#/daily-climate-data

Finkelstein, S. A., Doherty, C., & Loder, A. L. (2023). Safety Net Ontario: Ontario's outsized role in the "Global Safety Net" for climate and biodiversity. *FACETS*, *8*, 1–17. https://doi.org/10.1139/facets-2022-0126

Fraser, C. J. D., Roulet, N. T., & Moore, T. R. (2001). Hydrology and dissolved organic carbon biogeochemistry in an ombrotrophic bog. *Hydrological Processes*, *15*(16), 3151–3166. https://doi.org/10.1002/hyp.322

Freeze, R. A., & Cherry, J. A. (1979). *Groundwater*. Prentice-Hall.

Furukawa, A. K., Sutton, O. F., Simone, K. L., Verkaik, G. J., Moore, P. A., Clark, A., Fallas, R., Moore, M., Sherwood, E., Broyd, R. C., Van Huizen, B., Morris, P. J., & Waddington, J. M. (2025). Hydrological Feedbacks in Northern Peatlands 2: Peat Depth as a Control on Peatland Resilience. *Ecohydrology*, *18*(8), e70158. https://doi.org/10.1002/eco.70158

https://doi.org/10.5194/egusphere-2026-3284
Preprint. Discussion started: 19 June 2026

Glaser, P. H., Siegel, D. I., Reeve, A. S., Janssens, J. A., & Janecky, D. R. (2004a). Tectonic drivers for vegetation patterning and landscape evolution in the Albany River region of the Hudson Bay Lowlands. *Journal of Ecology*, *92*(6), 1054–1070. https://doi.org/10.1111/j.0022-0477.2004.00930.x

Glaser, P. H., Siegel, D. I., Reeve, A. S., Janssens, J. A., & Janecky, D. R. (2004b). Tectonic drivers for vegetation patterning and landscape evolution in the Albany River region of the Hudson Bay Lowlands. *Journal of Ecology*, *92*(6), 1054–1070. https://doi.org/10.1111/j.0022-0477.2004.00930.x

Goodbrand, A., Westbrook, C. J., & van der Kamp, G. (2019). Hydrological functions of a peatland in a Boreal Plains catchment. *Hydrological Processes*, *33*(4), 562–574. https://doi.org/10.1002/hyp.13343

Graniero, P. A., & Price, J. S. (1999). The importance of topographic factors on the distribution of bog and heath in a Newfoundland blanket bog complex. *CATENA*, *36*(3), 233–254. https://doi.org/10.1016/S0341-8162(99)00008-9

Harris, L. I., Richardson, K., Bona, K. A., Davidson, S. J., Finkelstein, S. A., Garneau, M., McLaughlin, J., Nwaishi, F., Olefeldt, D., Packalen, M., Roulet, N. T., Southee, F. M., Strack, M., Webster, K. L., Wilkinson, S. L., & Ray, J. C. (2022). The essential carbon service provided by northern peatlands. *Frontiers in Ecology and the Environment*, *20*(4), 222–230. https://doi.org/10.1002/fee.2437

He, H., Emilson, E., Balliston, N., Ledger, K., Barreto, C., Morison, M., Guzzi, A., Kuzyk, Z. Z., Papakyriakou, T., Bona, K., Cassidy, A., Hararuk, O., & Webster, K. (Submitted). Regional synthesis of Dissolved Organic Carbon for the Hudson Bay Lowlands. *Journal of Geophysical Research: Biogeosciences*. https://doi.org/2025JG009657-T

Hird, J. N., DeLancey, E. R., McDermid, G. J., & Kariyeva, J. (2017). Google Earth Engine, Open-Access Satellite Data, and Machine Learning in Support of Large-Area Probabilistic Wetland Mapping. *Remote Sensing*, *9*(12). https://doi.org/10.3390/rs9121315

Hoag, R. S., & Price, J. S. (1995). A field-scale, natural gradient solute transport experiment in peat at a Newfoundland blanket bog. *Journal of Hydrology*, *172*(1), 171–184. https://doi.org/10.1016/0022-1694(95)02696-M

Holden, J. (2005). Piping and woody plants in peatlands: Cause or effect? *Water Resources Research*, *41*(6). https://doi.org/10.1029/2004WR003909

https://doi.org/10.5194/egusphere-2026-3284
Preprint. Discussion started: 19 June 2026

Holden, J., & Burt, T. P. (2002). Piping and pipeflow in a deep peat catchment. *CATENA*, *48*(3), 163–199. https://doi.org/10.1016/S0341-8162(01)00189-8

Holden, J., Burt, T. P., & Vilas, M. (2002). Application of ground-penetrating radar to the identification of subsurface piping in blanket peat. *Earth Surface Processes and Landforms*, *27*(3), 235–249. https://doi.org/10.1002/esp.316

Holden, J., Smart, R. P., Dinsmore, K. J., Baird, A. J., Billett, M. F., & Chapman, P. J. (2012). Natural pipes in blanket peatlands: Major point sources for the release of carbon to the aquatic system. *Global Change Biology*, *18*(12), 3568–3580. https://doi.org/10.1111/gcb.12004

Howie, S. A., & van Meerveld, I. (H. J.). (2016). Classification of vegetative lagg types and hydrogeomorphic lagg forms in bogs of coastal British Columbia, Canada. *Canadian Geographer / Le Géographe Canadien*, *60*(1), 123–134. https://doi.org/10.1111/cag.12241

Hribljan, J. A., Kane, E. S., Pypker, T. G., & Chimner, R. A. (2014). The effect of long-term water table manipulations on dissolved organic carbon dynamics in a poor fen peatland. *Journal of Geophysical Research: Biogeosciences*, *119*(4), 577–595. https://doi.org/10.1002/2013JG002527

Hvorslev, M. J. (1951). *Time Lag and Soil Permeability in Ground-water Observations*. Waterways Experiment Station, Corps of Engineers, U.S. Army.

Ingram, H. a. P. (1978). Soil Layers in Mires: Function and Terminology. *Journal of Soil Science*, *29*(2), 224–227. https://doi.org/10.1111/j.1365-2389.1978.tb02053.x

Kazmiruk, Z. V., Capelle, D. W., Kamula, C. M., Rysgaard, S., Papakyriakou, T., & Kuzyk, Z. A. (2021). High biodegradability of riverine dissolved organic carbon in late winter in Hudson Bay, Canada. *Elementa: Science of the Anthropocene*, *9*(1), 00123. https://doi.org/10.1525/elementa.2020.00123

Khadka, B., Munir, T. M., & Strack, M. (2016). Dissolved organic carbon in a constructed and natural fens in the Athabasca oil sands region, Alberta, Canada. *Science of The Total Environment*, *557–558*, 579–589. https://doi.org/10.1016/j.scitotenv.2016.03.081

Kou, D., Virtanen, T., Treat, C. C., Tuovinen, J.-P., Räsänen, A., Juutinen, S., Mikola, J., Aurela, M., Heiskanen, L., Heikkilä, M., Weckström, J., Juselius, T., Piilo, S. R., Deng, J., Zhang, Y., Chaudhary, N., Huang, C., Väliranta, M., Biasi, C., … Shurpali, N. J. (2022). Peatland Heterogeneity Impacts on Regional Carbon

https://doi.org/10.5194/egusphere-2026-3284
Preprint. Discussion started: 19 June 2026

Flux and Its Radiative Effect Within a Boreal Landscape. *Journal of Geophysical Research: Biogeosciences*, *127*(9), e2021JG006774. https://doi.org/10.1029/2021JG006774

Lambert, C., Larocque, M., Gagné, S., & Garneau, M. (2022). Aquifer-Peatland Hydrological Connectivity and Controlling Factors in Boreal Peatlands. *Frontiers in Earth Science*, *10*. https://doi.org/10.3389/feart.2022.835817

Langlois, M. N., Price, J. S., & Rochefort, L. (2015). Landscape analysis of nutrient-enriched margins (lagg) in ombrotrophic peatlands. *Science of The Total Environment*, *505*, 573–586. https://doi.org/10.1016/j.scitotenv.2014.10.007

Laudon, H., Kuglerová, L., Sponseller, R. A., Futter, M., Nordin, A., Bishop, K., Lundmark, T., Egnell, G., & Ågren, A. M. (2016). The role of biogeochemical hotspots, landscape heterogeneity, and hydrological connectivity for minimizing forestry effects on water quality. *Ambio*, *45*(A2), 152–162. https://doi.org/10.1007/s13280-015-0751-8

Letts, M. G., Roulet, N. T., Comer, N. T., Skarupa, M. R., & Verseghy, D. L. (2000). Parametrization of peatland hydraulic properties for the Canadian land surface scheme. *Atmosphere-Ocean*, *38*(1), 141–160. https://doi.org/10.1080/07055900.2000.9649643

Li, Chen, H., White, J. C., Wulder, M. A., & Hermosilla, T. (2020). Discriminating treed and non-treed wetlands in boreal ecosystems using time series Sentinel-1 data. *International Journal of Applied Earth Observation and Geoinformation*, *85*, 102007. https://doi.org/10.1016/j.jag.2019.102007

Li, Han, D., Rogers, C. A., Finkelstein, S. A., Hararuk, O., Waddington, J. M., Barreto, C., McLaughlin, J. W., Snider, J., & Gonsamo, A. (2025a). Peat Depth and Carbon Storage of the Hudson Bay Lowlands, Canada. *Geophysical Research Letters*, *52*(2), e2024GL110679. https://doi.org/10.1029/2024GL110679

Li, Y., Han, D., Rogers, C. A., Finkelstein, S. A., Hararuk, O., Waddington, J. M., Barreto, C., McLaughlin, J. W., Snider, J., & Gonsamo, A. (2025b). Peat Depth and Carbon Storage of the Hudson Bay Lowlands, Canada. *Geophysical Research Letters*, *52*(2), e2024GL110679. https://doi.org/10.1029/2024GL110679

Limpens, J., Berendse, F., Blodau, C., Canadell, J. G., Freeman, C., Holden, J., Roulet, N., Rydin, H., & Schaepman-Strub, G. (2008). *Peatlands and the carbon cycle: From local processes to global implications – a synthesis*.

https://doi.org/10.5194/egusphere-2026-3284
Preprint. Discussion started: 19 June 2026

Liu, K.-B. (1990). Holocene Paleoecology of the Boreal Forest and Great Lakes-St. Lawrence Forest in Northern Ontario. *Ecological Monographs*, *60*(2), 179–212. https://doi.org/10.2307/1943044

Locky, D. A., Bayley, S. E., & Vitt, D. H. (2005). The vegetational ecology of black spruce swamps, fens, and bogs in southern boreal Manitoba, Canada. *Wetlands*, *25*(3), 564–582. https://doi.org/10.1672/0277-5212(2005)025%255B0564:TVEOBS%255D2.0.CO;2

McCarter, Kaufman, S., Branfireun, B., & Waddington, J. (2024). Peat swamp hydrological connectivity and runoff vary by hydrogeomorphic setting: Implications for carbon storage. *Ecohydrology*, *17*(3), e2637. https://doi.org/10.1002/eco.2637

McCarter, & Price, J. S. (2017). Experimental hydrological forcing to illustrate water flow processes of a subarctic ladder fen peatland. *Hydrological Processes*, *31*(8), 1578–1589. https://doi.org/10.1002/hyp.11127

McLaughlin, J. W., Lewin, J. C., Reed, D. D., Trettin, C. C., Jurgensen, M. F., & Gale, M. R. (1994). Soil Factors Related to Dissolved Organic Carbon Concentrations in a Black Spruce Swamp, Michigan. *Soil Science*, *158*(6), 454.

Moore, Didemus, B. D., Furukawa, A. K., & Waddington, J. M. (2021). Peat depth as a control on Sphagnum moisture stress during seasonal drought. *Hydrological Processes*, *35*(4), e14117. https://doi.org/10.1002/hyp.14117

Moore, H. E., Comas, X., Briggs, M. A., Reeve, A. S., & Slater, L. D. (2024). Indications of preferential groundwater seepage feeding northern peatland pools. *Journal of Hydrology*, *638*, 131479. https://doi.org/10.1016/j.jhydrol.2024.131479

Moore, T. R. (2009). Dissolved Organic Carbon Production and Transport in Canadian Peatlands. In *Carbon Cycling in Northern Peatlands* (pp. 229–236). American Geophysical Union (AGU). https://doi.org/10.1029/2008GM000816

Moore, T. R., Matos, L., & Roulet, N. T. (2003). Dynamics and chemistry of dissolved organic carbon in Precambrian Shield catchments and an impounded wetland. *Canadian Journal of Fisheries and Aquatic Sciences*, *60*(5), 612–623. https://doi.org/10.1139/f03-050

Morris, P. J., Davies, M. L., Baird, A. J., Balliston, N., Bourgault, M.-A., Clymo, R. S., Fewster, R. E., Furukawa, A. K., Holden, J., Kessel, E., Ketcheson, S. J., Kløve, B., Larocque, M., Marttila, H., Menberu, M. W., Moore, P. A., Price, J. S., Ronkanen, A.-K., Rosa, E., … Wilkinson, S. L. (2022). Saturated Hydraulic Conductivity

https://doi.org/10.5194/egusphere-2026-3284
Preprint. Discussion started: 19 June 2026

in Northern Peats Inferred From Other Measurements. *Water Resources Research*, *58*(11), e2022WR033181. https://doi.org/10.1029/2022WR033181

Morris, P. J., Waddington, J. M., Benscoter, B. W., & Turetsky, M. R. (2011). Conceptual frameworks in peatland ecohydrology: Looking beyond the two-layered (acrotelm–catotelm) model. *Ecohydrology*, *4*(1), 1–11. https://doi.org/10.1002/eco.191

National Wetlands Working Group. (1997). *The Canadian Wetland Classification System- Second Edition*. Wetlands Research Centre. https://nawcc.wetlandnetwork.ca/Wetland%20Classification%201997.pdf

NRCan. (2000). *Canadian Digital Surface Model* [Dataset]. Government of Canada Open Government Portal. https://app.geo.ca/en-ca/map-browser/record/768570f8-5761-498a-bd6a-315eb6cc023d

OMNRF. (2014). *Far North Land Cover* (Version V1.4) [Dataset]. ontario.ca

Packalen, M. S., Finkelstein, S. A., & McLaughlin, J. W. (2014). Carbon storage and potential methane production in the Hudson Bay Lowlands since mid-Holocene peat initiation. *Nature Communications*, *5*(1), 4078. https://doi.org/10.1038/ncomms5078

Pastor, J., Solin, J., Bridgham, S. D., Updegraff, K., Harth, C., Weishampel, P., & Dewey, B. (2003). Global warming and the export of dissolved organic carbon from boreal peatlands. *Oikos*, *100*(2), 380–386. https://doi.org/10.1034/j.1600-0706.2003.11774.x

Price, J., McCarter, C., & Quinton, W. (2023). *Groundwater in Peat and Peatlands | The Groundwater Project*. The Groundwater Project. https://doi.org/10.21083/978-1-77470-015-0.

Prijac, A., Gandois, L., Taillardat, P., Bourgault, M.-A., Riahi, K., Ponçot, A., Tremblay, A., & Garneau, M. (2023). Hydrological connectivity controls dissolved organic carbon exports in a peatland-dominated boreal catchment stream. *Hydrology and Earth System Sciences*, *27*(21), 3935–3955. https://doi.org/10.5194/hess-27-3935-2023

Quinton, W., & Roulet. (1998). Spring and Summer Runoff Hydrology of a Subarctic Patterned Wetland. *Arctic and Alpine Research*, *30*(3), 285–294.

Rezaeianzadeh, M., Kalin, L., & Hantush, M. M. (2018). An Integrated Approach for Modeling Wetland Water Level: Application to a Headwater Wetland in Coastal Alabama, USA. *Water*, *10*(7), 879. https://doi.org/10.3390/w10070879

https://doi.org/10.5194/egusphere-2026-3284
Preprint. Discussion started: 19 June 2026

Rezanezhad, F., Price, J. S., Quinton, W. L., Lennartz, B., Milojevic, T., & Van Cappellen, P. (2016a). Structure of peat soils and implications for water storage, flow and solute transport: A review update for geochemists. *Chemical Geology*, *429*, 75–84. https://doi.org/10.1016/j.chemgeo.2016.03.010

Rezanezhad, F., Price, J. S., Quinton, W. L., Lennartz, B., Milojevic, T., & Van Cappellen, P. (2016b). Structure of peat soils and implications for water storage, flow and solute transport: A review update for geochemists. *Chemical Geology*, *429*, 75–84. https://doi.org/10.1016/j.chemgeo.2016.03.010

Ritson, J. P., Brazier, R. E., Graham, N. J. D., Freeman, C., Templeton, M. R., & Clark, J. M. (2017). The effect of drought on dissolved organic carbon (DOC) release from peatland soil and vegetation sources. *Biogeosciences*, *14*(11), 2891–2902. https://doi.org/10.5194/bg-14-2891-2017

Rosset, T., Binet, S., Antoine, J.-M., Lerigoleur, E., Rigal, F., & Gandois, L. (2020). Drivers of seasonal- and event-scale DOC dynamics at the outlet of mountainous peatlands revealed by high-frequency monitoring. *Biogeosciences*, *17*(13), 3705–3722. https://doi.org/10.5194/bg-17-3705-2020

Roulet, N. T., Lafleur, P. M., Richard, P. J. H., Moore, T. R., Humphreys, E. R., & Bubier, J. (2007). Contemporary carbon balance and late Holocene carbon accumulation in a northern peatland. *Global Change Biology*, *13*(2), 397–411. https://doi.org/10.1111/j.1365-2486.2006.01292.x

Rydin, H., & Jeglum, K. (2013). *The Biology Of Peatlands Second Edition*. Oxford University press. https://www.slideshare.net/slideshow/the-biology-of-peatlands-second-edition-2nd-edition-hkan-rydin/280240060

Saurette, D., Warren, J., & Heck, R. (2018). 2.3: Soils of Ontario. In *Digging Into Canadian Soils: An Introduction to Soil Science*. Canadian Society of Soil Science. https://geo.libretexts.org/Bookshelves/Soil_Science/Digging_into_Canadian_Soils%3A_An_Introduction_to_Soil_Science/02%3A_Digging_Across_Canada/2.03%3A_Soils_of_Ontario

Schmidt, M. A., Santia, V., Price, S., Khumbani, H. A. W., & Strack, M. (2025). Quantifying Carbon Pools and Fluxes in Southern Ontario Temperate Swamps. *Mires and Peat*, *32*. https://doi.org/10.19189/001c.151276

Siegel, D. I., & Glaser, P. (2006). The Hydrology of Peatlands. In R. K. Wieder & D. H. Vitt (Eds.), *Boreal Peatland Ecosystems* (pp. 289–311). Springer. https://doi.org/10.1007/978-3-540-31913-9_13

https://doi.org/10.5194/egusphere-2026-3284
Preprint. Discussion started: 19 June 2026

Smart, R. P., Holden, J., Dinsmore, K. J., Baird, A. J., Billett, M. F., Chapman, P. J., & Grayson, R. (2013). The dynamics of natural pipe hydrological behaviour in blanket peat. *Hydrological Processes*, *27*(11), 1523–1534. https://doi.org/10.1002/hyp.9242

Solomon, C. T., Jones, S. E., Weidel, B. C., Buffam, I., Fork, M. L., Karlsson, J., Larsen, S., Lennon, J. T., Read, J. S., Sadro, S., & Saros, J. E. (2015). Ecosystem Consequences of Changing Inputs of Terrestrial Dissolved Organic Matter to Lakes: Current Knowledge and Future Challenges. *Ecosystems*, *18*(3), 376–389. https://doi.org/10.1007/s10021-015-9848-y

Sothe, C., Gonsamo, A., Arabian, J., Kurz, W. A., Finkelstein, S. A., & Snider, J. (2022). Large Soil Carbon Storage in Terrestrial Ecosystems of Canada. *Global Biogeochemical Cycles*, *36*(2), e2021GB007213. https://doi.org/10.1029/2021GB007213

Spence, C., & Woo, M. (2003). Hydrology of subarctic Canadian shield: Soil-filled valleys. *Journal of Hydrology*, *279*(1), 151–166. https://doi.org/10.1016/S0022-1694(03)00175-6

Strack, M., & Waddington, J. M. (2007). Response of peatland carbon dioxide and methane fluxes to a water table drawdown experiment. *Global Biogeochemical Cycles*, *21*(1). https://doi.org/10.1029/2006GB002715

Strack, M., Waddington, J. M., Bourbonniere, R. A., Buckton, E. L., Shaw, K., Whittington, P., & Price, J. S. (2008). Effect of water table drawdown on peatland dissolved organic carbon export and dynamics. *Hydrological Processes*, *22*(17), 3373–3385. https://doi.org/10.1002/hyp.6931

Sutton, O., Moore, P., Furukawa, A., Morris, P., & Waddington, J. (2025, March 18). *Shallow Peatlands as Sentinels of Climate Change*. https://doi.org/10.5194/egusphere-egu25-7613

Tiwari, T., Sponseller, R. A., & Laudon, H. (2022). The emerging role of drought as a regulator of dissolved organic carbon in boreal landscapes. *Nature Communications*, *13*, 5125. https://doi.org/10.1038/s41467-022-32839-3

Ulanowski, T. A., & Branfireun, B. A. (2013). Small-scale variability in peatland pore-water biogeochemistry, Hudson Bay Lowland, Canada. *Science of The Total Environment*, *454–455*, 211–218. https://doi.org/10.1016/j.scitotenv.2013.02.087

Urban, N. R., Bayley, S. E., & Eisenreich, S. J. (1989). Export of dissolved organic carbon and acidity from peatlands. *Water Resources Research*, *25*(7), 1619–1628. https://doi.org/10.1029/WR025i007p01619

https://doi.org/10.5194/egusphere-2026-3284
Preprint. Discussion started: 19 June 2026

Waddington, J. M., Morris, P. J., Kettridge, N., Granath, G., Thompson, D. K., & Moore, P. A. (2015). Hydrological feedbacks in northern peatlands. *Ecohydrology*, *8*(1), 113–127. https://doi.org/10.1002/eco.1493

Wallin, M. B., Grabs, T., Buffam, I., Laudon, H., Agren, Å., Öquist, M. G., & Bishop, K. (2013). Evasion of CO2 from streams—The dominant component of the carbon export through the aquatic conduit in a boreal landscape. *Global Change Biology*, *19*(3), 785–797. https://doi.org/10.1111/gcb.12083

Webster, K. L., Bhatti, J. S., Thompson, D. K., Nelson, S. A., Shaw, C. H., Bona, K. A., Hayne, S. L., & Kurz, W. A. (2018). Spatially-integrated estimates of net ecosystem exchange and methane fluxes from Canadian peatlands. *Carbon Balance and Management*, *13*(1), 16. https://doi.org/10.1186/s13021-018-0105-5

Werner, B. J., Lechtenfeld, O. J., Musolff, A., de Rooij, G. H., Yang, J., Gründling, R., Werban, U., & Fleckenstein, J. H. (2021). Small-scale topography explains patterns and dynamics of dissolved organic carbon exports from the riparian zone of a temperate, forested catchment. *Hydrology and Earth System Sciences*, *25*(12), 6067–6086. https://doi.org/10.5194/hess-25-6067-2021

Weyman, D. R. (1975). *Runoff processes and streamflow modelling*. Oxford University Press. https://library.wur.nl/WebQuery/titel/344316

Wilson, R. M., Hopple, A. M., Tfaily, M. M., Sebestyen, S. D., Schadt, C. W., Pfeifer-Meister, L., Medvedeff, C., McFarlane, K. J., Kostka, J. E., Kolton, M., Kolka, R. K., Kluber, L. A., Keller, J. K., Guilderson, T. P., Griffiths, N. A., Chanton, J. P., Bridgham, S. D., & Hanson, P. J. (2016). Stability of peatland carbon to rising temperatures. *Nature Communications*, *7*(1), 13723. https://doi.org/10.1038/ncomms13723

Yavitt, J. B. (1994). Carbon dynamics in Appalachian peatlands of West Virginia and Western Maryland. *Water, Air and Soil Pollution*, *77*(3), 271–290.

Zarov, E., Lapshina, E., Kuhlmann, I., & Schulze, E. D. (2023). Carbon Accumulation and the Possibility of Carbon Losses by Vertical Movement of Dissolved Organic Carbon in Western Siberian Peatlands. *Forests, Forest Species Distribution, Diversity and Growth under Climate Change*, *14*(12), 2393. https://doi.org/10.3390/f14122393